www.sciencemag.org/content/350/6261/663/suppl/DC1

Supplementary Materials for

The ecology of the microbiome: Networks, competition, and stability

Katharine Z. Coyte, Jonas Schluter,* Kevin R. Foster*

*Corresponding author. E-mail: jonas.schluter+sokendai@gmail.com (J.S.); kevin.foster@zoo.ox.ac.uk (K.R.F.)

Published 6 November 2015, *Science* **350**, 663 (2015)
DOI: 10.1126/science.aad2602

This PDF file includes:

Supplementary Materials

In the following we provide a detailed account of our analyses. The supplement is structured by methods; first linear stability analysis, second permanence analysis, third individual-based simulations, and fourth experimental validation. The contents are as follows:

Contents

Method 1

1a. Linear stability analysis

Our model considers networks of interacting species in which each species' growth is determined by its own intrinsic growth rate, interactions with other members of the same species, and interactions with members of other species. This is in accordance with previous models (*17, 18, 32*) and a generalization of classic Lotka-Volterra equations that allows us to incorporate multiple species and interaction types. Species are represented as densities averaging over many individuals – an approach that is well suited to the large population sizes of microbial species.

We analyze equilibrium populations and ask: will a population return to this equilibrium following a perturbation? This allows us to investigate the effect of different between-species interaction types on both the asymptotic stability of populations (*17*), and another measure of stability, the speed at which such a stable population returns to its equilibrium point (*48*). The former definition of stability has been applied widely to analyze fundamental properties of dynamical systems, and generates similar predictions to other measures of ecological stability, which ask whether any species will be lost from a system following perturbation (*37*). In later sections (Methods 2 and 3, below) we also consider alternative methods and definitions of stability, which show consistent results. Note that all our analyses are based on the logic of asking how community properties, like degree of connectedness or cooperation, affect ecological stability. This focus means we do not deal with the interesting corollary of how communities of a particular set of properties arise. However, we refer the reader to the literatures on both community assembly (*49*) and the evolution of species interactions (*50*) that focus on this question. In addition, we acknowledge that there is the potential for important interactions between these

processes and those that we study here, which are interesting targets for future work.

Our analytical approach is based upon calculating the eigenvalues of the Jacobian matrix of the dynamical system considered – a matrix that tells us how a change in the density of any of the species at equilibrium will affect the whole community. A population is asymptotically stable provided the real part of each of its associated eigenvalues lies below zero, and the community will return to its equilibrium following a small perturbation faster, the more negative its largest real part is. Both measures of stability, therefore, can be determined from the region in the complex plane to which all eigenvalues will be restricted, and we extend the recent analytic results of Allesina and Tang to derive these regions for an ecosystem with any potential mixture of interaction types (*18*). Specifically, we show that given certain assumptions about the distribution from which interaction strengths are drawn, eigenvalues will be localized within an ellipse in the complex plane with horizontal radius r_e, centered about $-s$. One single eigenvalue may be localized outside of this ellipse; we denote this by r_s which is given by the average row sum of the Jacobian matrix minus the average self interaction s. The equilibrium community will therefore be asymptotically stable provided both the ellipse and r_s lie within the negative real part of the complex plane, equivalent to,

$$\text{Rightmost point} = \max(r_e, r_s) - s < 0.$$

We can further deduce that the more negative this rightmost point is, the quicker the community will return to equilibrium, and thus the stability of the system can be determined from the negative of this rightmost value. We are therefore able to study the effect of changing various community characteristics upon stability by examining the subsequent effects upon this rightmost value. In the following we discuss in detail how the eigenvalue bounds can be derived.

Problem outline

Throughout this work, we consider a microbiota community composed of S interacting species, whose population dynamics are determined by a Holling type 1 functional response, such that the change in the density of species i is given by,

$$\frac{dX_i}{dt} = X_i(r_i - s_i X_i + \sum_{j=1, j\neq i}^{S} a_{ij} X_j). \tag{1}$$

Here r_i represents the intrinsic species growth rate, s_i captures the effect of a species upon itself, and a_{ij} the effect of species j upon species i (for $i \neq j$). We assume that each species competes to the same extent with members of their own species (i.e. resulting in the same degree of self-regulation), such that $s_i = s, i = 1, \ldots, S$. The connectivity $C \in [0, 1]$ of the community determines the fraction of all S species that a single species i interacts with (i.e., the average number of links between species such that $a_{i\neq j} \neq 0$)

We assume that non-zero interactions between species i and j can take one of five possible forms based on the signs of a_{ij}/a_{ji}; $+/-$ (exploitative), $-/-$ (competitive), $+/+$ (cooperative), $+/0$, and $-/0$. For a given community, the proportion of interactions taking each of these forms are defined as,

$$\begin{aligned} +/- &= P_e, \\ -/- &= P_c, \\ +/+ &= P_m, \\ +/0 &= P_+, \\ -/0 &= P_-, \\ \text{where } P_e + P_c + P_m + P_+ + P_- &= 1. \end{aligned}$$

Following the same approach as Chen and Cohen and others (*18, 32, 37*), we assume the system has a positive definite equilibrium given by the $S \times 1$ vector $\mathbf{X}^*$. This is equivalent to examining the system

$$\frac{dY_i}{dt} = Y_i(r_i + q_{ii}Y_i + \sum_{j=1, j\neq i}^{S} q_{ij}Y_j),$$

normalized by replacing each y_i by $x_i = \frac{y_i}{q_i}$. We ignore systems that do not have a positive definite equilibrium, as they will automatically be deemed unstable by our definition, and contradict experimental evidence suggesting equilibrium communities in the gut exist for extended periods of time. We can therefore determine the stability of a thus normalized equilibrium point by examining the distribution of the eigenvalues of the Jacobian of the system, evaluated at $\mathbf{X}^*$, whose entries are given by,

$$\begin{aligned} A_{ii} &= -s_i, \quad i = 1, \ldots, S \\ A_{ij} &= a_{ij}, \quad i, j = 1, \ldots, S. \end{aligned}$$

Derivation of stability criterion

The basis of our stability criterion can be traced back to the seminal work by Gerschgorin, who showed for a complex $S \times S$ matrix M with elements m_{ij} that each eigenvalue λ_i lies within at least one of S Gerschgorin disks, which are centered at the diagonal entries (m_{ii}) with radii

$$R_i = \sum_{j=1, j\neq i}^{S} |a_{ij}|,$$

(*51*). This was used by Sommers *et al* in 1988 (*30*), who examined the eigenvalues of an $S \times S$ matrix M^* with elements drawn from a Normal distribution with mean,

$$\begin{aligned} \mathbb{E}(M_{ij}^*) &= 0, \\ Var(M_{ij}^*) &= \frac{1}{S}, \\ M_{ii}^* &= 0. \end{aligned}$$

The authors proved that as $S \to \infty$ then the eigenvalues of M^* will be distributed on an ellipse described by $(\frac{x}{a})^2 + (\frac{y}{b})^2 \leq 1$ centered at the origin, with $a = 1 + \tau$ and $b = 1 - \tau$ where $\tau = S\mathbb{E}(M_{ij}^* M_{ji}^*)$. Allesina and Tang (*18*), motivated by Tao *et al.* (*52*), showed that this conclusion is also applicable to non-Normal distributions, save for one eigenvalue that is approximately equal to the average row sum of M^*, and further noted that setting each of the diagonal entries a_{ii} to $-s$ will move the center of this ellipse to $(-s, 0)$, thus the system will be stable if the half-horizontal radius of the eigenvalue ellipse is less than s.

Here we follow a similar approach to that used in (*18*), and use various rescaling arguments to derive a bound upon the eigenvalues of the Jacobian, A, corresponding to our dynamical system of the microbiota evaluated at the equilibrium $\mathbf{X}^*$ for any mixture of different interaction types. We assume that between-species interaction strengths a_{ij} are drawn from a half Normal distribution $|N(0, \sigma^2)|$ such that the mean strength of realized interactions is given by $\mathbb{E}(|X|) = \sqrt{\frac{2\sigma^2}{\pi}}$, and the variance $Var(|X|) = \sigma^2\Big(1 - \frac{2}{\pi}\Big)$.

When S is large, the row sum of A is constant and equal to

$$\lim_{S\to\infty} m = S^{-1} \sum_{i,j=1;i\neq j}^{S} a_{ij},$$

thus $\mathbf{1}$ is an eigenvector of A. The mean of the off-diagonal entries of A, $E(A_{ij}) = m$, and thus A does not meet the requirements of Sommers's theorem, so we next define a new matrix $N = A + (-s + m)I - m.\mathbf{1}.\mathbf{1}^T$. Rothblum and Tan showed that for any $m \in \mathbb{R}$, the half horizontal radius of the eigenvalue ellipse for the matrix $N = A + (-s + m)I - m.\mathbf{1}.\mathbf{1}^T$ will

have the same value as the half horizontal radius for A (*18, 53*). We can therefore calculate a bound on the distribution of the eigenvalues of A by first calculating the distribution of the eigenvalues of N.

We begin by taking into account the different interaction types present in our community, and decompose the mean of the off-diagonal entries according to these different types. The average off-diagonal row sum for mixed interaction type matrices is then given by,

$$\begin{aligned}\mathbb{E}(A_{ij}) &= C(P_m\mathbb{E}(|X|) - P_c\mathbb{E}(|X|) + 0.5P_+\mathbb{E}(|X|) - 0.5P_-\mathbb{E}(|X|)),\\ &= C\mathbb{E}(|X|)(P_m - P_c + 0.5(P_+ - P_-)),\end{aligned}$$

and we note that $m = \mathbb{E}(A_{ij})$, and the matrix N is therefore,

$$\mathbb{E}(N_{ij}) = \mathbb{E}(A_{ij} - m) = \mathbb{E}(A_{ij}) - m = 0,$$

such that N and any scalar multiple of this matrix will obey the first requirement of Sommers's theory, i.e. $\mathbb{E}(cN) = 0, c \in \mathbb{R}$. We next consider the variance of N, $Var(N_{ij}) = Var(A_{ij} - m)$. As m is simply a constant, we have,

$$\begin{aligned}Var(N_{ij}) &= Var(A_{ij}),\\ &= \mathbb{E}(A_{ij}^2) - \mathbb{E}(A_{ij})^2.\end{aligned}$$

Further, using the fact that $P_e + P_c + P_m + P_+ + P_- = 1$, and the definition of the second moment of the half-normal distribution from which the A_{ij}s are drawn, we have,

$$
\begin{aligned}
\mathbb{E}(A_{ij}^2) &= C(P_m\mathbb{E}(A_{ij}^2) + P_c\mathbb{E}(A_{ij}^2) + P_e\mathbb{E}(A_{ij}^2) + 0.5P_+\mathbb{E}(A_{ij}^2) + 0.5P_-\mathbb{E}(A_{ij}^2)), \\
&= C\mathbb{E}(A_{ij}^2)(1 - 0.5P_+ - 0.5P_-), \\
&= C\sigma^2(1 - \frac{P_+ + P_-}{2}), \text{and therefore,} \\
Var(N_{ij}) &= C\sigma^2(1 - \frac{P_+ + P_-}{2}) - m^2. \qquad (2)
\end{aligned}
$$

We next rescale N, setting $N^* = \frac{N}{\beta}$ with $\beta = \sqrt{SVar(N_{ij})}$, such that the matrix N^* fulfills both of the requirements of Sommers's theory. That is:

$$
\begin{aligned}
\mathbb{E}(N^*) &= 0, \\
Var(N^*) &= \frac{1}{S}.
\end{aligned}
$$

Thus all eigenvalues of N^* will be contained in the ellipse with half-horizontal radius $a^* = 1 + \tau$ and half-vertical radius $b^* = 1 - \tau$ with $\tau = \mathbb{E}(N_{ij}^* N_{ji}^*) = \frac{\mathbb{E}(N_{ij}N_{ji})}{\beta^2}$. Further, we note that eigenvalues are closed under scalar multiplication, thus if λ is an eigenvalue of the matrix N^*, then $\beta\lambda$ will be an eigenvalue of N. This means that the eigenvalues of N will be contained in the ellipse with half-horizontal radius $a = \beta(1 + \tau)$ and half-vertical radius $b = \beta(1 - \tau)$. This gives us a bound on the half-horizontal radius of the ellipse containing the eigenvalues of N, and therefore of A of:

$$
r_e = \sqrt{SVar(N_{ij})}\Big(1 + \frac{S\mathbb{E}(N_{ij}N_{ji})}{SVar(N_{ij})}\Big). \qquad (3)
$$

We must then calculate $\mathbb{E}(N_{ij}N_{ji})$, which we do by noting that:

$$\begin{aligned}\mathbb{E}(N_{ij}N_{ji}) &= \mathbb{E}(A_{ij}A_{ji}) - 2m\mathbb{E}(A_{ij}) + m^2, \\ &= \mathbb{E}(A_{ij}A_{ji}) - m^2\end{aligned} \tag{4}$$

where,

$$\begin{aligned}\mathbb{E}(A_{ij}A_{ji}) &= C(P_m\mathbb{E}(A_{ij}A_{ji}|+/+) + P_c\mathbb{E}(A_{ij}A_{ji}|-/-) + \dots \\ &\quad P_e\mathbb{E}(A_{ij}A_{ji}|+/-) + P_+\mathbb{E}(A_{ij}A_{ji}|+/0) + P_-\mathbb{E}(A_{ij}A_{ji}|-/0)), \\ &= C(P_m\mathbb{E}(A_{ij}A_{ji}|+/+) + P_c\mathbb{E}(A_{ij}A_{ji}|-/-) + P_e\mathbb{E}(A_{ij}A_{ji}|+/-)), \\ &= C(P_m\mathbb{E}(|X|)^2 + P_c\mathbb{E}(|X|)^2 - P_e\mathbb{E}(|X|)^2), \\ &= C\mathbb{E}(|X|)^2(2(P_m+P_c) + P_+ + P_- - 1).\end{aligned}$$

We can substitute (2) and (4) into (3) to give the expression for the half-horizontal radius of the eigenvalue ellipse of A as:

$$\begin{aligned}r_e &= \sqrt{SC(\sigma^2(1-\frac{P_+ + P_-}{2}) - C\mathbb{E}(|X|)^2(P_m - P_c + \frac{P_+ - P_-}{2})^2)}\dots \\ &\quad \Big(1 + \frac{\mathbb{E}(|X|)^2((2P_m + 2P_c + P_+ + P_- - 1) - C(P_m - P_c + 0.5P_+ - 0.5P_-)^2)}{\sigma^2(1 - 0.5P_+ - 0.5P_-) - C\mathbb{E}(|X|)^2(P_m - P_c + 0.5P_+ - 0.5P_-)^2}\Big)\end{aligned}$$

Finally, we observe that the eigenvalue corresponding to the average row sum will be given by,

$$r_s = (S-1)C(P_m - P_c + \frac{P_+ - P_-}{2})\mathbb{E}(|X|).$$

From these we generate a stability criterion for a network with any mixture of interaction types,

$$\max(r_e, r_s) - s < 0.$$

1b. Analysis of stability criterion

The analyses presented in the main paper suggest that cooperation has a destabilizing influence on microbial communities (Figure 2). Here we provide supplementary analyses of our model to show that this prediction holds for the vast majority of conditions and parameters in our analytical model. We first show that cooperation has a universally destabilizing effect on exploitative or random communities for any realistic combinations of species number and connectivity. We then analyze the effect of cooperation on purely competitive networks. Here, increasing cooperation nearly always destabilizes communities except for a minor parameter range where increased cooperation can have a weakly stabilizing effect. Moreover, as we show below, the weakly stabilizing effect is further minimized when we consider realistic communities with a mixture of competitive and exploitative interactions.

To determine how cooperation affects community stability we take the derivative of our measure of stability, U, with respect to P_m. This tells us how stability changes with respect to the level of cooperation - with a negative derivative meaning cooperation decreases stability. We can therefore examine the effect of cooperation by looking at the sign of this derivative, $\frac{dU}{dP_m}$, across parameter space.

In the analysis below we treat each type of community (exploitative / random / competitive) separately, and follow the same series of steps. For simplicity we consider communities with only $+/+$, $-/-$, and $+/-$ interactions, however, the same analysis can equivalently be extended to cover communities that also contain $+/0$ and $-/0$ interactions. We begin by recalling that stability of a community at equilibrium is defined as the negative of the rightmost bound upon its underlying eigenvalues (that is, communities whose eigenvalues lie further to the right in the complex plane are less stable), which are contained within an ellipse centered at $-s$ with half-horizontal radius,

$$
\begin{aligned}
r_e &= \sqrt{SVar(N_{ij})}\Big(1+\frac{\mathbb{E}(N_{ij}N_{ji})}{Var(N_{ij})}\Big), \\
&= \sqrt{SC(\sigma^2 - C\mathbb{E}(|X|)^2(P_m-P_c)^2)}\ldots \\
&\quad \Big(1+\frac{\mathbb{E}(|X|)^2((2P_m+2P_c-1)-C(P_m-P_c)^2)}{\sigma^2 - C\mathbb{E}(|X|)^2(P_m-P_c)^2}\Big),
\end{aligned} \tag{5}
$$

save for a single eigenvalue that may lie outside the ellipse, and is approximated by,

$$
r_s = -s + (S-1)C(P_m-P_c)\mathbb{E}(|X|). \tag{6}
$$

Stability is therefore defined as $U = -(\max(r_e - s, r_s))$. As such, the derivative of stability, $\frac{dU}{dP_m}$ will be defined differently, depending upon whether the ellipse or the dot represents the rightmost bound. In our analysis, we therefore calculate separately the derivative of the ellipse, $\frac{dU^{ellipse}}{dP_m}$, and of the dot, $\frac{dU^{dot}}{dP_m}$, then for each combination of P_m, C, and S check which component is governing stability for that parameter set, to determine the appropriate derivative. We then plot a heatmap across parameter space, to indicate in which regions cooperation is stabilizing ($\frac{dU}{dP_m} > 0$) and in which it is destabilizing ($\frac{dU}{dP_m} < 0$).

We begin by noting that in all community types, the self-regulation, s, does not affect the impact of cooperation upon community stability and so our conclusions on how cooperation influences stability are general for all values of self-regulation. Specifically, in our measure of stability the self-regulation is a constant, independent of P_m, and as such, it does not appear in $\frac{dU}{dP_m}$ (equivalently, note that $\frac{d^2U}{dP_m ds} = 0$ for both the ellipse and the dot). Moreover, whilst increasing species number, S, will increase the magnitude of the role cooperation plays upon community stability, it will not affect the directionality - thus if we find that increasing cooperation is destabilizing, increasing species number will not affect this conclusion. This can be seen from the derivative of $\frac{dU}{dP_m}$ with respect to S for the ellipse and dot. For the ellipse,

$$\frac{d^2U}{dP_m dS} = \frac{-1}{2\sqrt{S}}\frac{d}{dP_m}\Big(\sqrt{Var(N_{ij})}\Big(1+\frac{\mathbb{E}(N_{ij}N_{ji})}{Var(N_{ij})}\Big)\Big),$$

and so only the magnitude of the effect of increasing cooperation upon stability is affected. Specifically, the magnitude will decrease with the inverse of the square root of S when the ellipse governs stability. Similarly for the dot,

$$\frac{d^2U}{dP_m dS} = -\frac{d}{dP_m}C(P_m - P_c),$$

which is constant over S, so again only the magnitude of the effect of cooperation upon stability is affected. Crucially, these observations mean that any conclusions drawn about the effect of increasing cooperation upon stability for low species number will also hold for all larger communities (and any value of self-regulation). As such, in our analysis we can set species number and self-regulation to constants, $S = 100$ and $-s = -1$ respectively, and focus exclusively upon whether changing connectivity, C, will affect the role of cooperation upon stability.

Exploitative communities

We start by considering the case of increasing cooperation in communities in which all interactions are otherwise exploitative ($+/-$). In this case there are never any competitive interactions, so we substitute $P_c = 0$ into our equations for stability, (5) and (6). We then take the derivative of each with respect to P_m to get the equation for the ellipse bound,

$$\frac{dU^{ellipse}_{exploit}}{dP_m} = -\frac{CS^{\frac{1}{2}}\mathbb{E}(|X|)^2(2C^2P_m^3\mathbb{E}(|X|)^2 - CP_m\mathbb{E}(|X|)^2 - 3CP_m\sigma^2 + 2\sigma^2)}{(-CP_m^2\mathbb{E}(|X|)^2 + \sigma^2)\sqrt{C(\sigma^2 - CP_m^2\mathbb{E}(|X|)^2)}},$$

and for the dot,

$$\frac{dU^{dot}_{exploit}}{dP_m} = -(S-1)C\mathbb{E}(|X|).$$

It is evident from the form of $\frac{dU^{dot}}{dP_m}$ that in cases where the dot governs community behavior stability will decrease linearly with cooperation. However, the form of $\frac{dU^{ellipse}}{dP_m}$ is less obvious, and we therefore plot $\frac{dU}{dP_m}$ across C/P_m parameter space for a community with 100 species (Figure S4). This illustrates how cooperation will always decrease stability ($\frac{dU}{dP_m}$ is always negative) and moreover, as explained above, this behavior will hold true for any equivalent communities with differing levels of self-regulation or greater species numbers. Figure S4 also illustrates how this destabilizing effect of increasing cooperation upon the community will be stronger in communities with higher network connectivity.

Random communities

We next examine the effect of increasing cooperation in communities that are otherwise random. In these communities networks start with cooperative, exploitative, and competitive interactions in a $1:2:1$ ratio. As cooperation increases, exploitative and competitive interactions are replaced with equal probability, such that exploitation : competition remains at a ratio of $2:1$. To capture this, we substitute $P_c = \frac{1}{3}(1-P_m)$ in equations (5) and (6). We then take the derivative of each with respect to P_m to calculate the derivative for the ellipse,

$$\frac{dU^{ellipse}_{rand}}{dP_m} = \frac{4CS^{\frac{1}{2}}\mathbb{E}(|X|)^2\Big(2C^2\mathbb{E}(|X|)^2(64P_m^3-48P_m^2+12P_m-2)-27\sigma^2(4CP_m-C-1)\Big)}{3(9C\sigma^2-C^2\mathbb{E}(|X|)^2(4P_m-1)^2)^{1/2}(\mathbb{E}(|X|)^2(16CP_m^2-8CP_m+C)-9\sigma^2)},$$

and for the dot,

$$\frac{dU^{dot}_{rand}}{dP_m} = -\frac{4}{3}(S-1)C\mathbb{E}(|X|).$$

Again it is clear by inspection that when community behavior is determined by the dot, stability will decrease linearly with cooperation, and at a greater rate than for exploitative communities (the value of $\frac{dU^{dot}_{rand}}{dP_m}$ is constant and less than that of $\frac{dU^{dot}_{exploit}}{dP_m}$). As in the exploitative case, we plot $\frac{dU}{dP_m}$ across C/P_m for $S = 100$ (Figure S5). Again we see that in this case cooperation is always destabilizing, regardless of whether the dot or the ellipse determines community behavior (the derivative is always negative), and as outlined above, this will hold for any level of self-regulation and any larger communities. Moreover, again it is evident that this destabilizing effect is greater for communities with higher network connectivity.

Competitive communities

Finally we consider increasing cooperation in systems that are otherwise purely competitive, so substitute $P_c = 1 - P_m$ in equations (5) and (6). As before, we take the derivative of each with respect to P_m to find the change with cooperation to the ellipse,

$$\frac{dU^{ellipse}_{compete}}{dP_m} = \frac{2C^2S^{\frac{1}{2}}\mathbb{E}(|X|)^2(2P_m-1)(\mathbb{E}(|X|)^2(2C+1+8CP_m(P_m-1))-3\sigma^2)}{((C\sigma^2-C^2\mathbb{E}(|X|)^2(2P_m-1)^2))^{1/2}(4CP_m\mathbb{E}(|X|)^2(P_m-1)+C\mathbb{E}(|X|)^2-\sigma^2)},$$

and to the dot,

$$\frac{dU^{dot}_{compete}}{dP_m} = -2C\mathbb{E}(|X|)(S-1).$$

As before, we observe that when the behavior of the community is determined by the dot, stability will decrease linearly with cooperation, and at a rate twice as fast as equivalent exploitative communities. However, in this case, we find regions of C/P_m parameter space where increasing cooperation can in fact have a stabilizing effect upon the community (that is, $\frac{dU}{dP_m} > 0$), as illustrated by Figure S6. However, the magnitude of this effect is small such that it will rarely make an unstable system stable (Figure S6 C). Moreover, this effect is further

reduced when one considers more realistic communities that contain even just small amounts of exploitative interactions such that the total proportion of cooperative and competitive links are no longer kept constant (Figure S6 D – F). From these analyses, we conclude that cooperation between species is a destabilizing influence on ecological stability for the vast range of network compositions, species numbers, and connectivities.

1c. Independent scaling of interaction types

In order to study the effects of host manipulation (Figure 4), we want to independently scale the interaction strengths within communities. In this section, we outline how this is done. For simplicity, below we derive our new stability criterion with only $+/-$, $-/-$, and $+/+$ interactions. However, the same methods could be applied to also incorporate $+/0$ and $-/0$ interactions. We begin by weighting interactions such that the average magnitude of each interaction type is given by,

$$\begin{aligned} f\mathbb{E}(|X|) \quad &\text{for} \quad +/+, \\ g\mathbb{E}(|X|) \quad &\text{for} \quad -/-, \\ h\mathbb{E}(|X|) \quad &\text{for} \quad +/-, \end{aligned}$$

whilst self-regulation will now take the form $-s * k$. The mean of the off-diagonal entries of the Jacobian will now be given by,

$$\mathbb{E}(A_{ij}) = C\mathbb{E}(|X|)(fP_m - gP_c),$$

and similarly, the variance and covariance by,

$$
\begin{aligned}
Var(A_{ij}) &= C\sigma^2(f^2P_m + g^2P_c + h^2(1 - P_m - P_c)) - C^2\mathbb{E}(|X|)^2(fP_m - gP_c)^2, \\
\mathbb{E}(A_{ij}A_{ji}) &= C(f^2P_m\mathbb{E}(|X|)^2 + g^2P_c\mathbb{E}(|X|)^2 - h^2(1 - P_m - P_c)\mathbb{E}(|X|)^2).
\end{aligned}
$$

We can then use the same logic as in supplementary section 1 to get an expression for the half-horizontal radius of the ellipse,

$$
\begin{aligned}
r_e^w &= \sqrt{SC(\sigma^2(f^2P_m + g^2P_c + h^2(1 - P_m - P_c)) - C\mathbb{E}(|X|)^2(fP_m - gP_c)^2)}\ldots \\
&\quad \Big(1 + \frac{\mathbb{E}(|X|)^2(P_m(f^2 + h^2) + P_c(g^2 + h^2) - h^2 - C(fP_m - gP_c)^2)}{\sigma^2(f^2P_m + g^2P_c + h^2(1 - P_m - P_c)) - C\mathbb{E}(|X|)^2(fP_m - gP_c)^2}\Big),
\end{aligned}
$$

and the average row sum,

$$
r_s^w = C(S - 1)\mathbb{E}(|X|)(fP_m - gP_c).
$$

From these our stability criterion for a network with any mixture of interaction types, each of which can now be weighted independently, is given by

$$
\max(r_e^w, r_s^w) - sk < 0.
$$

With this we can now investigate how different manipulations to the microbiota will affect the stability of the community. Specifically, we consider three distinct cases: in the first, we consider spatial structure that reduces between-species interactions while self-regulation stays the same, corresponding to a decrease in f, g, and h, whilst k remains the same (Figure 4). In the second, we consider the case where a host provides a generic food source with which all microbes interact instead of interacting with each other, corresponding to a decrease in f, g, h and k (down-weighting all interaction types, Figure S12). In the final case, only cooperative links are weakened by host nutrient secretion, for example when a nutrient source is diverting

interaction efforts away from cross-feeding interactions towards consumption of host provided nutrients. This corresponds to a decrease in f only (Figure 4). See methods 2 and 3 below for further analyses of these three cases.

1d. Effect of host-mediated killing on community stability

The immune system is thought to act, via inflammation and other mechanisms, to help suppress pathogens or other species that reach densities where they are harmful to a host (*3–5, 23*). We can capture this effect in our model as species-specific density dependent killing at a rate k_i where,

$$\begin{aligned} \frac{dX_i}{dt} &= X_i(r_i - s_i X_i + \sum a_{ij} X_j - k_i X_i), \\ &= X_i(r_i - s_i^* X_i + \sum a_{ij} X_j), \end{aligned} \tag{7}$$

with $s_i^* = s_i + k_i$. As such, density dependent killing acts in the same way as self-regulation, which has a stabilizing effect on the community.

We can also ask what happens should the host kill members of each species at a constant rate independent of the population sizes. Here, we observe no change in the stability of communities. Killing does put extra demands on community members, it will favor faster growing community members that can survive in the face of the killing. But for viable communities that can persist in the face of the killing, there is no net effect on ecological stability. This can be seen incorporating a global increased death rate in our model. The term r_i is the intrinsic growth rate of species i, which is a combination of the rates of birth, b_i, and death, d_i, of cells of species i, that is, $r_i = b_i - d_i$. In the absence of general host killing, stable communities with a given set of interactions, a_{ij}, fulfil,

$$r_i = s_i^* X_i - \sum a_{ij} X_j.$$

If the host kills members of each species at a constant rate, k_i, then this will be incorporated into our original system describing community dynamics as,

$$\begin{aligned} \frac{dX_i}{dt} &= X_i(r_i^* - s_i X_i + \sum a_{ij} X_j) - k_i X_i, \\ &= X_i((r_i^* - k_i) - s_i X_i + \sum a_{ij} X_j), \end{aligned} \tag{8}$$

Species members of a stable community must now have an intrinsic growth rate, r^*, such that,

$$r^* = s_i X i - \sum a i j X_j + k_i.$$

A community will therefore have to possess a stronger intrinsic growth rate when subject to a constant level of killing to be viable. However, we note that,

$$r^* - k_i = s_i X_i - \sum a i j X_j = r_i,$$

such that the equations governing the dynamics of both populations are in fact identical, regardless of the level of killing, and thus will have an identical probability of being stable. While the evolution of non-responsive killing may cause shifts in which species are able to make a viable community, therefore, we find no net effect on the stability of the communities that can persist in the face of the killing.

1e. Effect of redundancy on community stability

Our models indicate that the instability of highly cooperative communities stems from having strong positive dependencies between species. What happens though if the interactions between cooperating partners is less specific and, instead of interacting strongly with few partners, co-operators interact weakly with several partners? Such redundancy is common in biological

networks and we want to understand its effects here. One simple effect of such redundancy will be to weaken the strength of cooperative links, which has a stabilizing effect (supplement section 1b). However, redundancy is also expected to increase the number of interactions. For example, rather than interacting with one species with an interaction strength of $a_{ij} = 1$, a species may instead interact with 3 others, where each interaction now has strength $\frac{1}{3}$.

We capture this in our analytic model with the parameter q, which represents the average number of new links that each original cooperative link is replaced with. Each new link has, on average, a strength $a_{ij}q$, where a_{ij} represents the strength of the original interaction. As redundancy increases so too will the connectivity of the community, C^{new}, as well as the overall proportion of cooperation, P_m^{new}. However, concurrently the average strength of cooperative interactions, and interactions in the community as a whole, will decrease. These changes are captured by,

$$\begin{aligned} C^{\text{new}} &= C^I(P_m^I q + P_c^I) \\ Pm^{\text{new}} &= \frac{qP_m^I}{qP_m^I + P_c^I} \end{aligned} \tag{9}$$

Where P_m^I, P_c^I, and C^I represent the initial levels of cooperation, competition, and connectivity respectively.

We can then examine the effect of increasing redundancy in communities with different initial levels of cooperation (Figure S13). We find that redundancy does not affect communities that start with high levels of cooperation, as any stabilizing effects of reduced link strength are canceled out by equivalent increases in the levels of cooperation and connectivity. However, in communities that begin with intermediate levels of cooperation, the stabilizing effect of reduced interaction strengths outweigh the destabilizing effects of increased cooperation and connectivity. To conclude, when redundancy means that cooperators interact with several other species

weakly rather than few species strongly, ecological stability can increase.

1f. Numerical simulations of representative communities

In the sections below we present two fundamentally different methods for analysing ecological stability: permanence analysis and individual-based modelling. However, we first directly confirm our analytical method by simulating representative networks and explicitly calculating the eigenvalues of the corresponding Jacobians. As above, we consider the generalized Lotka-Volterra model with S species outlined in (1), and now follow the same approach as (*32*) and (*18*), whereby each species intrinsic growth rate r_i is solved for so as to ensure a feasible equilibrium at $\mathbf{X} = \mathbf{1}$. The corresponding Jacobians will therefore have off-diagonal entries $J_{ij} = a_{ij}$, and diagonal entries $J_{ii} = -s_i$. We can then construct representative Jacobians as follows.

We first create an $S \times S$ matrix M with our desired connectivity, C. For each interaction pair (M_{ij}, M_{ji}) we draw a random variable p_1 from a Uniform $U([0,1])$ distribution, if $p_1 \leq C$ then we set M_{ij} and $M_{ji} = 1$, else, both are set to 0. We next impose the relevant distribution of interaction types on this network, where P_m represents the proportion of cooperative, $+/+$, interactions, P_c the proportion of competitive, $-/-$, interactions, and $1 - P_m - P_c$ the proportion of exploitative, $+/-$, interactions (for simplicity we confine ourselves to these types, however, this method can easily be extended to also incorporate $+/0$ and $-/0$ interactions). For each non-zero interaction pair (those where M_{ij} and $M_{ji} = 1$) we draw a new random variable p_2 from a $U([0,1])$ distribution. If $p_2 \geq 1 - P_m$ then (M_{ij}, M_{ji}) represents a cooperative interaction, and we draw values for the entries of our Jacobian J_{ij} and J_{ji} from a half-normal distribution $|N(0, \sigma^2)|$. If $p_2 \leq P_c$ then (M_{ij}, M_{ji}) represents a competitive interaction, and we draw the entries J_{ij} and J_{ji} from a negative half-normal distribution $-|N(0, \sigma^2)|$. If $P_c < p_2 < 1 - P_m$ then (M_{ij}, M_{ji}) represents an exploitative interaction, in this case we draw a further random variable

p_3 from a $U([0,1])$ distribution. If $p_3 \leq 0.5$ then species i benefits from the interaction whilst species j suffers and we draw J_{ij} from an $|N(0,\sigma^2)|$ distribution and J_{ji} from an $-|N(0,\sigma^2)|$ distribution. If $p_3 > 0.5$ then the converse is true, and we draw J_{ij} from an $-|N(0,\sigma^2)|$ distribution and J_{ji} from an $|N(0,\sigma^2)|$ distribution. Finally, we set each diagonal entry J_{ii} to $-s$. Thus we are able to generate Jacobians corresponding to networks with any mix of different interaction types, then solve to find the corresponding eigenvalues using Matlab (Mathworks, Natick, MA, USA).

The effects of feeding or spatial segregation on network stability are incorporated through altering the strengths of the interactions between species. Here, representative Jacobians are generated as outlined above, then, in the case of general feeding, all entries of the Jacobian are reduced by the weighting factor, in the case of targeted feeding, only the Jacobian entries corresponding to cooperative interactions are reduced, and in the case of spatial segregation, all Jacobian entries except for those on the diagonal, J_{ii}, are reduced.

1g. Comparison with previous numerical work

In this section we analyze a recent study of macroscopic communities by Mougi and Kondoh (*32*) to show that our analytical method can recapitulate the behaviour of previous numerical analyses. In addition, we explain the relationship of our predictions to (*32*), as we reach different conclusions owing to our focus on microbial communities. Both our work and that of (*32*) investigate the stability of a community of S species whose dynamics are described by the system of Lotka-Volterra equations,

$$\frac{dX_i}{dt} = X_i(r_i - s_i X_i + \sum_{j=1, j\neq i}^{N} a_{ij} X_j).$$

Here X_i is the density of species i, r_i its intrinsic growth rate, s_i the strength of self-regulation, and a_{ij} the effect of species j on i. A proportion C of possible interactions between species are realized, and these interactions are split such that P_m are cooperative $(+/+)$ and $P_c = 1 - P_m$ are exploitative $(+/-)$. Our work also allows for $-/-, +/0,$ and $-/0$ interactions, however, for comparison, we here limit ourselves to just $+/+$ and $+/-$ interactions.

Mougi and Kondoh numerically simulated communities with varying proportions of interaction types, and showed an increase in ecological stability for intermediate levels of cooperation (intermediate P_m). However, we find a monotonic decrease in ecological stability as cooperation is increased. Here we show that the finding of peak stability at intermediate cooperation is a consequence of specific assumptions in (*32*) on how organisms in macroscopic communities function. As we discuss below, these assumptions are unlikely to generally apply to microbial communities. Nevertheless, we show here that our analytic approach can recapitulate these earlier numerical results.

The key assumption can be understood in terms of a focal species having a separate "capacity" (time budget) for each of its interaction types. Consider, for example, an ant species that is in in a mutualism with an acacia plant. Mougi and Kondoh assign the ant species a separate time budget for a) the exploitative interactions with other species and b) the cooperative interactions with other species. As a result, if the ant species takes on more mutualistic partners, a second acacia species, it is assumed that the strength of its interaction with the original plant is weakened but, critically, the strength of its interaction with prey species is not weakened. Therefore, if one adds more cooperative (mutualistic) interactions to a network, it will down-weight only the cooperative interactions, and if one adds more exploitative (predator) interactions to a network it will down-weight only the exploitative interactions. However, this particular form of weighting, by interaction type, does not have a clear application to microbial

communities. Interactions between microbial species can readily switch from cooperative to exploitative (or competitive) in a manner that is inconsistent with each interaction type being a distinct enterprise with its own capacity. For example, a bacterial mutualism can change to another interaction type if a focal species simply stops providing a metabolite for another, or if the focal species up-regulates the production of an antibiotic (*50*). Such switches - effectively from a mutualist to a predator - highlight that different interaction types function within a single capacity, and give no justification for the weighting scheme illustrated with the ants and acacias above. And, as we show next, this assumption is key to the conclusion that community stability peaks at an intermediate proportion of cooperative interactions.

Mathematically, the weighting assumption is described by,

$$a_{ij} = \frac{e_i f_M A_{ij}}{\sum_{k \in \text{resources of mutualist } i} A_{ik}},$$

for cooperative (mutualistic) interactions, and,

$$\begin{aligned} a_{ij} &= \frac{g_i f_A A_{ij}}{\sum_{k \in \text{resources of predator } i} A_{ik}} \text{ and} \\ a_{ji} &= -\frac{f_A A_{ji}}{\sum_{k \in \text{resources of predator } i} A_{ik}}, \end{aligned}$$

for the predator and prey respectively in an exploitative interaction. Here A_{ij} represents the potential preference of species i to interact with species j, whilst e_{ij} and g_{ij} describe the efficiency of cooperative (mutualistic) and exploitative (predatory) interactions respectively. Each of these variables are drawn from Uniform $U(0,1)$ distributions with means $E(A_{ij}) = A$, $E(e_{ij}) = e$ and $E(g_{ij}) = g$. f_M and f_A describe the relative importance of mutualism versus predation, although these are simply set to $f_M = f_A = 1$ (*32*). In the limit of large S, C, and P_m this can be approximated by,

$$\begin{aligned}
\text{Mutualistic, } (+/+)\ a_{ij} &= \frac{f_M e_{ij} A_{ij}}{P_m(S-1)CA}, \\
\text{Predation, } (+/-)\ a_{ij} &= \frac{f_A g_{ij} A_{ij}}{0.5 P_e(S-1)CA}, \\
\text{Prey, } (-/+)\ a_{ij} &= \frac{-f_A A_{ij}}{0.5 P_e(S-1)CA}.
\end{aligned}$$

In their supplementary material, Mougi and Kondoh showed numerically that the increase in stability at intermediate levels of cooperative interactions was not present when omitting this weighting in networks with a cascade structure. In Figures S7 and S8 we first confirm numerically that the increase in stability at intermediate levels of cooperation also disappeared without the frequency dependent scaling of interaction strength in unstructured networks, such as our microbial networks. We next derive a stability criterion that captures frequency-dependent scaling of interaction strengths analytically. We determine stability by analyzing the Jacobian, M corresponding to this system, whose off-diagonal entries are given by $M_{ij} = a_{ij}X_i$, whilst the on-diagonal entries are simply $M_{ii} = -s_i X_i$. In the following derivation, we assume a constant level of self-regulation and equilibrium species densities, such that $X_i = X \forall i$ and $s_i = s \forall i$. The general results still hold when these factors are also drawn from probability distributions, but the ellipses become less accurate.

We use the same analysis employed when deriving our previous stability criteria, which hinges upon the observation made by Sommers (*30*), that a matrix N with mean 0, variance $\frac{1}{S}$, and correlation $E(N_{ij}N_{ji})$ (the mean of the product of all entries) centered at 0 will have eigenvalues uniformly distributed within an ellipse $(x/a)^2 + (y/b)^2 \leq 1$ where $a = 1 + \tau, b = 1 - \tau$ and τ is defined as $\tau = SE(N_{ij}N_{ji})$. Further, Rothblum and Tan showed that the only affect of adding the matrix $m\mathbf{1}.\mathbf{1}^{\mathbf{T}}$ to N will be to change the eigenvalue, λ^*, corresponding to the average row sum and the eigenvector $\mathbf{1}$ (which will become $\lambda + Sm$). Finally, adding a constant factor d to each diagonal entry of the matrix will simply shift all eigenvalues by d

along the real axis, such that each $\lambda_i = \lambda_i + d$. Thus, whilst the Jacobian, M, corresponding to our equilibrium community does not meet the requirements of Sommers's work, the network $N^* = \frac{N}{\sqrt{(SVarN))}}$, with $N = M - E(M)$, does, and therefore, the eigenvalues of our Jacobian will be contained within the ellipse centered at $-sX$, with half-horizontal radius, a, and half-vertical radius, b, given by,

$$a = \sqrt{SVar(N)}\Big(1 + \frac{E(N_{ij}N_{ji})}{Var(N)}\Big), \tag{10}$$

$$b = \sqrt{SVar(N)}\Big(1 - \frac{E(N_{ij}N_{ji})}{Var(N)}\Big). \tag{11}$$

We now derive expressions for $Var(N)$ and $E(N_{ij}N_{ji})$ in terms of the various community parameters (S, C, and the proportions of interaction types), such that we can determine how the eigenvalue distribution, and therefore stability, of our community varies as these parameters change. We first note that the mean of our Jacobian is given by,

$$\begin{aligned} E(M_{ij}) &= C\Big(P_m E(M_{ij}|+/+) + 0.5P_e E(M_{ij}|+/-) + 0.5P_e E(M_{ij}|-/+)\Big), \\ &= C\Big(P_m \frac{f_M e X}{P_m(S-1)C} + 0.5P_e \frac{f_A g X}{0.5P_e(S-1)C} - 0.5P_e \frac{f_A X}{0.5P_e(S-1)C}\Big), \\ &= \frac{X}{(S-1)}\Big(f_M e + f_A(g-1)\Big), \end{aligned}$$

and the second moment $E(M_{ij}^2)$ by,

$$\begin{aligned} E(M_{ij}^2) &= C\Big(P_m E(M_{ij}^2|+/+) + 0.5P_e E(M_{ij}^2|+/-) + 0.5P_e E(M_{ij}^2|-/+)\Big), \\ &= C\Big(P_m \frac{f_M^2 e_2 A_2 X^2}{(P_m(S-1)CA)^2} + 0.5P_e \frac{f_A^2 g_2 A_2 X^2}{(0.5P_e(S-1)CA)^2} \cdots \\ &\quad + \frac{f_A^2 A_2 X^2}{(0.5P_e(S-1)CA)^2}\Big), \\ &= \frac{X^2 A_2}{C(S-1)^2 A^2}\Big(\frac{f_M^2 e_2}{P_m} + \frac{2f_A^2(g_2+1)}{P_e}\Big). \end{aligned}$$

Where A_2, e_2 and g_2 are the second moments of A_{ij}, e_{ij} and g_{ij}, $A_2 = E(A_{ij}^2)$, $e_2 = E(e_{ij}^2)$ and $g_2 = E(g_{ij}^2)$ respectively. We can then calculate the variance of M, which is also the variance of $N = M - E(M_{ij})$, such that,

$$Var(M) = Var(N) = \frac{X^2}{C(S-1)^2}\Big(\frac{f_M^2 e_2 A_2}{P_m A^2} + \frac{2f_A^2(g_2+1)A_2}{P_e A^2} - C(f_M e + f_A(g-1))^2\Big). \quad (12)$$

From Sommers's theorem, we next require $E(N_{ij}N_{ji}) = E(M_{ij}M_{ji}) - E(M)^2$, for our stability criterion, and note that,

$$\begin{aligned} E(M_{ij}M_{ji}) &= C\Big(P_m E(a_{ij}a_{ji}X_iX_j| + /+) + P_e E(a_{ij}a_{ji}X_iX_j| + /-)\Big), \\ &= C\Big(P_m \frac{f_M^2 e^2 X^2}{(P_m(S-1)C)^2} - P_e \frac{4f_A^2 g X^2}{(P_e(S-1)C)^2}\Big), \\ &= \frac{X^2}{C(S-1)^2}\Big(\frac{f_M^2 e^2}{P_m} - \frac{4f_A^2 g}{P_e}\Big). \end{aligned}$$

We can, therefore, calculate the correlation of N,

$$E(N_{ij}N_{ji}) = \frac{X^2}{C(S-1)^2}\Big(\frac{f_M^2 e^2}{P_m} - \frac{4f_A^2 g}{P_e} - C(f_M e + f_A(g-1))^2\Big). \quad (13)$$

Combining this with equations (12) and (13) in (10) and (11) allows us to determine the coordinates of our eigenvalue ellipse. As before, there will also be an eigenvalue that corresponds to the eigenvector $\mathbf{1}$ which does not necessarily lie within the ellipse, and is approximately equal to the average row sum, in this case equal to,

$$\begin{aligned} \text{Row sum} &= C(S-1)\Big(P_m \frac{f_M X e}{C(S-1)P_m} + 0.5P_e \frac{f_A X g}{0.5P_e C(S-1)} - 0.5P_e \frac{f_M X}{0.5P_e C(S-1)}\Big), \\ &= X(f_M e + f_A(g-1)). \end{aligned}$$

We can then see analytically how the distribution of eigenvalues changes as we increase the proportion of cooperative interactions, P_m, for the frequency-dependent weighted and unweighted cases. For example, in Figure S9, we plot the numerical stability (line) and average maximum eigenvalue from 10 networks, showing how our distributions match, and we reproduce the phenomenon of peak stability for intermediate P_m under the assumption of frequency-dependent, interaction specific weighting of interaction strengths.

Method 2

2a. Permanence analysis

We next consider a different method to analyze the ecological stability of communities. Permanence analysis asks whether a community will retain all its members, independent of the scale of any perturbation. Mathematically, this means that the boundary of the state space – the points where one or more species have gone extinct – behaves as a repeller, such that if the densities of any of the species within the community approach zero, these species will not collapse but instead grow, meaning no trajectory of the system leads to the extinction of any species. In contrast to the analytics that can deal with large community sizes, permanence analysis is computationally expensive and so we will analyze small communities with $S = 10$ and where interactions are either $+/+$ or $-/-$ in varying proportions. As we discuss below, permanence analysis also has further restrictions in applicability such that it may under-estimate the proportion of permanent communities. Nevertheless, permanence analysis remains a much more complete study of the stability properties of a network, which makes it a valuable complement to the analytics. Moreover, despite its restrictions, we will show that it leads to the same conclusions as the analytical model and, subsequently, our individual-based model.

A sufficient condition for permanence was derived by Jansen in 1987 (*38*). This derivation

requires that not only must no species go extinct, but that it is not possible for any species to grow infinitely. In mutualistic Lotka-Volterra systems this is not always the case – some communities have the propensity for positive-feedbacks to drive species growth in such a way that some species will never stop growing. These situations are clearly unrealistic as microbiota populations will at least be capped by limited space within the gut. As this kind of cap is difficult to capture with first order differential equations, we investigate the effects of space limitation using an individual-based model (see supplementary section 3), and develop constraints for our permanence analysis so as to guarantee that we only analyze communities where infinite growth is not possible, while classifying those communities that permit infinite growth as non-permanent.

Specifically, the permanence analysis of a given community can be broken into the following parts. First, as in previous sections, we use Lotka Volterra equations to find a feasible equilibrium for the whole community by solving for the growth rates r using $X = \mathbf{1}$ (supplementary section 1a). We next check whether the community is unbounded – if the community is not bounded, and therefore has the capacity for infinite growth we classify it as non-permanent. If the community is bounded, we next check whether the boundary of the state space is also a repeller – if so then no species will ever go extinct, nor will any ever grow to infinity, and thus we classify the community as permanent. We outline these steps in more detail below.

2b. Boundedness of cooperative communities

In communities of mixed competitive and cooperative interactions, any growth towards infinity will be driven by the cooperative components of the community. Therefore, if the purely cooperative subsystem of a mixed community is bounded above then so too will be the mixed community.

In a purely cooperative community, interactions are described by an interaction matrix that is

negative on the diagonal and non-negative elsewhere. Such a matrix is termed a Metzler matrix, and it has been shown that if a dynamical system described by a Metzler matrix is locally stable, then the it will also be globally stable (*54*). This means that, if a feasible equilibrium point of a purely cooperative community is globally stable, this community will be bounded, such that no species will grow to infinity. We can therefore determine whether a mixed community is bounded above by checking whether the cooperative subsystem of the community is locally stable.

To check the boundedness of a given community described by the matrix J, we therefore first determine the cooperative subsystem of the community by removing all competitive between species interactions – setting all the negative off-diagonal elements of J to zero, to create a new community matrix J^*. We then solve for a new equilibrium X^*, using the new community matrix J^*. J^* is now a Metzler matrix, as all diagonal entries are negative ($= -s$, $s > 0$) and all off-diagonal entries are non-negative. Therefore, if the new equilibrium is feasible, i.e. $X_i^* > 0$ for all i, and locally stable, i.e. the largest real part of the eigenvalues of J^* at equilibrium is negative, then we categorize the whole community as bounded.

Note, while global stability is a sufficient condition for boundedness, it is not necessary. This means we may underestimate the number of permanent communities as we discard those partially cooperative communities that do not permit a globally stable equilibrium yet do not grow to infinity. However, this confines our permanence analysis to bounded communities, and we employ the individual-based model to directly study properties of communities that we here classify as unbounded and non-permanent (Method 3, below).

2c. Permanence of bounded communities

The necessary conditions for permanence in Jansen's work yields the following linear programming problem (*38*):

Minimize z subject to:

$$\sum_{i=1}^{S} h_i(r_i - s_i X_i^{B(k)} + \sum_{j=1, j\neq i}^{S} a_{ij} X_j^{B(k)}) + z \geq 0.$$

and $h_i > 0$ for all $i = 1, .., S$.

The h_i and z are variables of the linear programming problem taking into account the constraints arising from all feasible boundary equlibria X^B indexed by $k = 1, .., m$, where $m \leq 2^S$. We here perform permanence analysis in communities where $S = 10$. All other parameters and values, and the assembly of community matrices are the same as in the previous sections of this work with the exception that for the analysis of permanence, we choose a smaller self-regulation parameter, s. The small networks that we are studying here using permanence analysis are intrinsically more stable than the more realistically-large networks that we studied with the analytics above. All networks would simply be stable if we used the same self-regulation parameter as above. In order to study the effects of cooperation and other factors on stability, therefore, we lower s to 0.2 for the permanence analysis. Host manipulations such as feeding or spatial segregation are implemented as scaling factors for the entries of the Jacobian matrix, i.e. $a_{ij} \times f - 1$ where f is the strength of host manipulation. We simulate 200 independent communities for each set of parameters and plot the frequency of permanent systems.

Method 3

3a. Individual-based model

In addition to our permanence analysis, to verify our analytical work we also developed an individual-based model (IbM) of the microbiome. This cellular automaton explicitly models all cells in the community, and tracks their growth, death, and spatial location over time. The computationally intensive nature of our IbM limits the number of species that we are able to

investigate, and in accordance with our permanence analysis, we again set species number $S = 10$.

This approach offers several important pieces of information. First, whilst our other models focus on the binary question of whether or not an equilibrium community will be stable to perturbation, this approach gives us added information as to how we expect a community to behave following perturbation, and allows us to track population sizes of all species over time. Additionally, we can explicitly take into account spatial structuring of a community. This allows us to more directly examine the effect of spatially segregated communities upon community stability. Similarly, we can more explicitly examine the effect of host-supplied nutrients on the manner in which cells interact with one another, and the subsequent effects on stability. Additionally, this approach introduces the realistic stochasticity of birth and death events, and cell-cell interactions.

As in our analytical work, we consider a community of S species, where species interact with one another with probability C (consistent with our previous work, here $C = 0.7$ throughout). These interactions may be competitive, exploitative, or cooperative (the model can also easily be extended to incorporate commensalism and ammensalism), and are defined by an interaction matrix, A. The interaction strengths are initially drawn from a half normal $|N(0, \sigma^2)|$ distribution. We then scale A such that overall a discrete approximation of the Jacobian associated with the community at equilibrium is of a similar magnitude and distribution to that of our analytic work. Although each cell has a spatial location, we initially assume that diffusion in the environment is high, such that each cell can interact with every other cell within the environment. However, when we study the effects of spatial structure, cell interactions are constrained to a region around each cell (below).

We model the environment as a square lattice with periodic boundary conditions and sides of size N, such that the environment can contain a maximum of N^2 cells (throughout, $N = 100$).

However if the population exceeds a certain cap (in our case, 90% of the maximum population size) then a random selection of cells are removed to reduce the overall population size to the level of the cap – this can be thought of as a density dependent sloughing that imposes an upper limit on population size whilst still enabling cells to grow.

Unless stated otherwise, each simulation begins by seeding the environment such that it is 80% full (initial population size $0.8 \times N^2$), with each species composed of a roughly equivalent number of cells, distributed at random. Once the environment has been seeded, we count the starting number of each species, and set this as our initial equilibrium point, X_{eq}. We then solve to find the intrinsic growth rate if each species, r_i, necessary to maintain this equilibrium,

$$r = -(A \times X_{eq}).$$

Simulations then consist of the following series of steps, described in further detail below.

1. Count how many cells of each species are present in the environment at the start of the time point, contained in the vector X_t.

2. Calculate the growth rate for each species as dependent on X_t. In our initial simulations, all cells of the same species will grow at the same rate.

3. Randomly list all of the cells present in the environment, consider each cell in turn according to this order.

4. Instigate growth / death of each cell depending upon its species' growth rate and whether there are free spaces such that growth is possible.

At the start of each time point we count the total number of each species, X_t, then calculate the growth / death rate of each species, defined by,

$$\text{growthRates} = r + AX_t - \text{diag}(A).$$

The $-\text{diag}(A)$ term removes the interaction of each specific cell with itself while maintaining interactions with other cells of the same species. We next rescale all the rates to be between $[0, 1]$ by dividing each rate by the magnitude of the maximum growth / death rate at that time point. This gives us an adaptive time-step that enables us to distinguish between species with very small differences in growth rates.

We next list all cells in random order, then assign an independent $U([0, 1])$ random number, q, to each cell. We consider each cell in the list in turn. For each cell, if its growth rate is positive and greater than its assigned random number, q, we assume growth will occur, and a new cell of the same type will be placed in an adjacent spot (up, down, left, or right, chosen at random). If there are no free spots immediately adjacent to the focal cell, then no growth occurs. Similarly, if the cell's growth rate is negative, and its magnitude greater than its assigned random number, q, then we assume death occurs, and that cell is removed from the environment.

Once each cell has been considered, we check to see whether the population has grown over the pre-defined population cap, and if so we remove a randomly chosen set of cells, such that the population is reduced down to the population cap. This marks the end of the time-point, and the process repeats again.

We initially allow the simulation to run for five time-steps, then perturb the community – reducing the population size of each species by 10%. The simulation process then returns to run as normal for 1000 time-steps, and we evaluate the stability of the community following this perturbation. Specifically, we define stability as the proportion of communities that retain all their initial species throughout the simulation.

3b. Effect of cooperation on community stability

We begin by investigating how changing the proportion of cooperation within a community affects its stability. As in our analytic work, we achieve this by altering the interaction matrix, A, to change the proportion of cooperative interactions. We investigate this in three different settings – increasing cooperation in initially purely competitive communities, in purely exploitative ones, and in communities where interactions are otherwise randomly assigned.

3c. Effect of spatial segregation on community stability

We are interested in what potential mechanisms the host might possess to promote a stable microbiome. As discussed in the main text, one possible mechanism is spatial segregation, whereby the host reduces the probability of species interacting with one another. Specifically, we consider a case where populations start from a varying initial density and then grow clonally to create patches of a single genotype. The lower the density of the initial inoculation, the stronger the spatial structure (figure S14). Moreover, whilst in our original simulations we assumed that each cell could interact with every other cell, we now assume that each cell only interacts with a subset of cells within a certain radius of it.

As in our initial simulations, we define the capacity for interactions between species by the $S \times S$ matrix A, the parameters of which are drawn from a half normal $|N(0, \sigma^2)|$ distribution, with signs chosen so as to achieve the desired levels of cooperation, competition, and exploitation. We next take the distribution of cells described above, and set this as our equilibrium community, and solve for the intrinsic growth rate of each cell necessary to achieve this. Due to the addition of spatial structure and limited interaction neighborhood each cell will interact with a different subset of the population, so we must now calculate the growth rate of each cell individually. We define the vector X_i^{nb} as the number of of cells of each species within the neighborhood of cell i. We then calculate the growth rate for cell i as,

$$r^i = -(A(l, \text{all}). * X^i_{nb}),$$

where l is the species type of cell i. For each species we then average the growth rates, r_i, of all the cells of that type, and set this as the intrinsic growth rate for that species. The simulations then progress in the same manner as in our first, non-structured model; the cells are randomly ordered, their growth rates calculated, then any action (growth / death) implemented according to this random order. Unlike our original simulations where all cells of the same species had the same instantaneous growth rate, each cell will now have a different overall growth rate depending upon the subset of the population that lies within its neighborhood. As in our initial simulations, we run the model for five time steps before perturbing all of the species densities, then observe the ability of the community to retain all of its initial species over time.

3d. Effect of feeding on community stability

Hosts further manipulate their microbiome via epithelial feeding of microbes within the gut community. Here we extend our simulations to capture this behavior, and examine the consequences for community stability. We focus on two potential effects of host provision of nutrients upon the behavior of the gut community – first, the scenario whereby host provided nutrients act as an alternative nutrient sources for the gut microbes, and second, the case in which nutrients act as an extra source of energy by which to increase cell growth rates. We discuss each of these approaches in detail below.

Case 1: food as an alternative to interactions

One potential effect of host-provided nutrients is that they act as an alternative to bacteria-provided substrates – that is, the use of a host supplied nutrient weakens the interactions between the microbes in the community. For example, the host supplied nutrient may be an alter-

native carbon source to a nutrient supplied by another community member. This case is directly analogous to the case explored in our analytic work (Figures 4 B, S12). Here, we explore two possible options; in the first all interactions between cells can potentially be weakened by interacting with the host supplied nutrients (general feeding, Figure S12) whilst, in the second, host supplied nutrients only have the effect of weakening interactions between cooperative species (targeted feeding, Figure 4 B). In both cases we assume that each species' initial equilibrium density is determined from a combination of both its interactions with other microbes and with the host supplied nutrient.

In our simulation we capture this with the presence of an additional nutrient source, kept at a constant level, which can be metabolized by members of the gut community. Like cells themselves, this nutrient has a spatial component, and will only weaken interactions when a cell overlaps with the location of the nutrient. We define the effect of using the nutrient, ϕ, (here $\phi = 10^{-5}$ so as to be on the same order of magnitude as a single cell-cell interaction in our models) and the simulation is then composed of the following steps, listed below.

As in our initial simulations, the process begins by seeding the environment with roughly equal numbers of each species, placed at random (without any structure), and setting this distribution as the community equilibrium. In the same manner, set quantities of nutrients are also placed at random in the environment (to be redistributed each timestep). We set γ to be the proportion of cells that will on average overlap in location with nutrient molecules, and of this, δ represents the proportion of these overlaps in which, on average, nutrients are metabolized in favor of an interaction with neighboring cells. This equates to whether cells have a preference for interacting with other microbes (when $\delta < 0.5$), or with the host provided nutrients (when $\delta > 0.5$). We then use this to calculate the intrinsic growth rates, r, of each species as,

$$r = -(A(X_{eq} - \delta\ \gamma\ X_{eq}) + 1\delta\ \phi\ \gamma\ N^2),$$

so as to set the initial population as the community equilibrium. The simulation then follows the same series of steps to our previous implementations of the model.

Case 2: Food as a supplement to cell-cell interactions

We next investigate the scenario where host-provided nutrients acts as an extra resource that acts in addition to pre-existing microbial interactions. In this case we consider a population that is already at equilibrium, then study the effect of adding nutrients to the environment. As in Case 1, we begin by seeding the environment with a random distribution of each species, and a set amount of nutrients. We then calculate the intrinsic growth rates of each species, r, independent of any nutrients present in the environment, such that,

$$r = -(A(X_{eq})).$$

Each time-step then begins by counting the population size of each species, contained in X, then calculating each species' growth rate, now given by,

$$\text{growthRates} = r + AX - diag(A) + \phi\,\gamma\,N^2,$$

where as before ϕ represents the strength of an interaction with the host supplied nutrients, and γN^2 the number of nutrient molecules that each cell interacts with. As such, the last term on the right represents the contribution to the overall growth rate from interactions with host-supplied nutrient molecules. As before, growth rates are rescaled by the magnitude of the maximum rate of cell growth or death in the community, cells ordered at random, then each cell considered in turn, with any actions (growth / death / nothing) decided based on the value of their species' growth (or death) rate.

When the additional nutrients provided by the host remain at a constant level throughout the simulation, this increases intrinsic growth rates (growth not dependent upon microbial interac-

tions) and therefore reduces the likelihood of species going extinct. By the measure of stability used to analyze our IbM results – whether a community is able to maintain all of its initial species over time, feeding therefore acts to increase the stability of the microbial community (Figure 4 C). This is a different form of stability to that above. As is typical in the literature, our earlier analyses consider communities maintained at a stable equilibrium by the interactions between the community members. However, the effect of increased growth rates here is to push the species' populations to their maximum size, such that they are now regulated extrinsically by the capacity of the host. This is critical because it can turn what were formerly cooperating species into competitors.

To see this, it is important to realize that the occurrence of competition versus cooperation can be more nuanced than simply examining the interaction parameters (a_{ij}) between species in the model. In the presence of an external population cap, these interaction terms only define the net effects of one species on another during early stages of growth, before the community has reached the cap. However, once the community has reached its steady state at the cap, the effect of one species on another is now a combination of both the direct interaction terms (a_{ij}) and competition for limited space. This latter effect can change previously cooperative interactions into competitive ones.

The change to competition can be demonstrated in our model by removing a previously cooperative species and observing how this removal affects the other species. If the focal species is cooperating, removing it should harm the other species (*50*). However, removing the focal species, we see that the other species typically both increase in their densities and their rate of cell production per unit time (Figure 4 C). The removed species was then, at this point, primarily a competitor with negative effects on most other species.

4. Experimental validation

While there is a rapidly growing body of data on species abundances in the mammalian microbiome, there have been few studies focused on deciphering the interactions between these species. However, the work by Stein *et al.* (*16*) is one such study. The authors used time-resolved metagenomics and machine learning to infer the interactions between community members – species or genera – within a mouse model. These data then allowed us to test our predictions about the profile of ecological interactions within the mammalian microbiome.

We first looked at the distribution of interaction types between the community members. Our analysis predicts that a stable community within the microbiome will contain only a small proportion of destabilizing cooperative interactions, amongst a larger number of competitive or exploitative links. We found that this is indeed the case in the Stein *et al.* dataset (Figure 4 D, bar chart), in which of all possible interactions, only 14.8 % are cooperative.

A second key prediction from our analysis is that, in a stable microbial community, the interactions between species should be predominantly weak relative to the self-regulation that each species experiences due to within-species competition, captured by s (see equation S1). Again we find our prediction is supported by the Stein et al. data – the histogram in Figure 4 D shows how the vast majority of ecological interactions between community members are weaker than that of the average interaction of a species with itself ($\bar{s}$), with only a few strong ecological interactions between members.

The models we have presented here are general, which makes them widely applicable and able to identify general principles. However, a criticism of such models is that generality might come at a cost of accuracy if important details are not accounted for. Do our models then make correct predictions when we parameterize them using real data? We evaluated this question using the Stein *et al.* data. Specifically, we obtained the general community parameters – $S, C, P_m, P_c, \sigma, \bar{s}$ – of a stable mouse microbiome community from Stein*et al.* Using these in

our analytical model (supplementary section 1) we can predict the bound on the eigenvalues, and therefore the stability, of this community. Not only did our analysis correctly predict the community to be stable, but we also correctly estimated the location of the stability determining dominant eigenvalue in the community when this value was explicitly calculated using each individual member's densities and interaction strengths (Figure 4 D, right).

Supplementary Figures

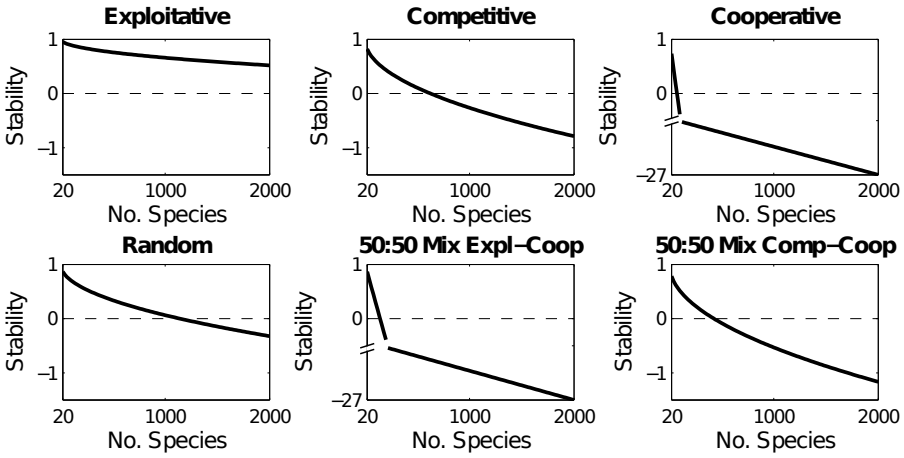

Figure S1: **Diversity destabilizes communities**. Here we plot our analytic measure of stability over increasing species number for random networks with different interaction types ($C = 0.7, -s = -1, \sigma = 0.05$). Increasing the species number has destabilizing effects across communities of all interaction types. Mathematically, adding new species to a network in this way always increases the largest real part of the community's eigenvalues and, therefore, the stability of the community decreases. The higher the proportion of positive interactions within the community, the larger this effect - and thus diversity is most destabilizing for cooperative communities. Note that we use a break in the y axis of some plots in order to allow the early behaviour of all plots to be directly compared.

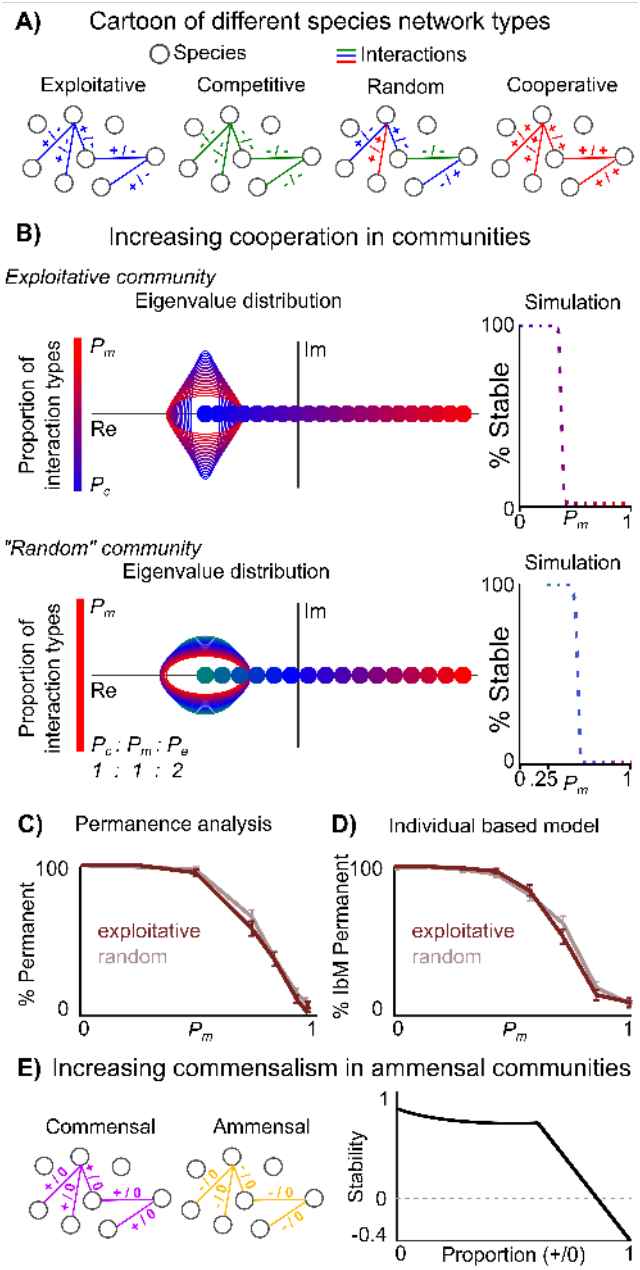

Figure S2: **Increased proportions of cooperative interactions decrease stability in exploitative and random communities.** A) Illustration of different network types; competitive (green), exploitative (blue), random, and cooperative (red). B) Linear stability analysis. Left hand plot shows analytical solutions for eigenvalue locations as a function of increasing cooperation (shown as increasing red). The largest value of the real components (x-axis) determines whether, and how fast, a return to equilibrium occurs (stability), whilst the imaginary components (y-axis) determine the frequency of oscillations in population densities following perturbations (Figure 1). The solutions give the position of all eigenvalues in the form of an ellipse, with the exception of a single eigenvalue that corresponds to the average row sum of the interaction matrix (represented by a dot that may lie outside of the ellipse). Increasing cooperation increases the largest eigenvalues, and stability decreases. Solutions hold for any permutation of a community network with a given parameter set (here: $S = 100$, $C = 0.7$, $-s = -1$, $\sigma = 0.05$, see supplementary section 1b for parameter sweeps that show that cooperation is nearly always destabilizing). Right hand plots are simulation results showing the proportion of communities that are stable to confirm our analytic results. C, D) Increasing cooperation also decreases community stability in our permanence analysis and individual-based model (here: $S = 10$, $C = 0.7$, $-s = -0.2$, $\sigma = 0.05$, errorbars: SEM for 100 samples). E) Increasing commensalism $(+/0)$ within an ammensal $(-/0)$ community has a similarly destabilizing effect.

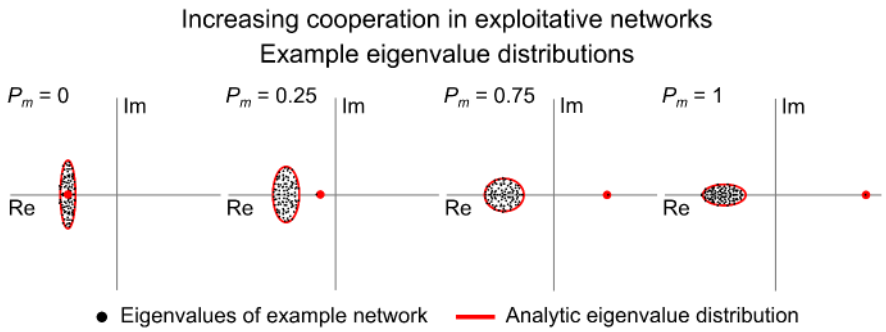

Figure S3: **Numerical confirmation of the analytical model for increasing cooperation in an exploitative community**. The stability of a community is dependent upon the localization of its eigenvalues within the complex plane, which we can predict using our analytic measure. We confirm the accuracy of this analytical approach by simulating representative communities ($S = 100, C = 0.7, -s = -1, \sigma = 0.05$) and explicitly calculating their eigenvalues (black dots), which we can see are contained within our analytically calculated bound (red, Figure 2). For example, we confirm that stability decreases (the largest real eigenvalue part becomes less negative) when we increase the proportion of cooperation in an otherwise exploitative network.

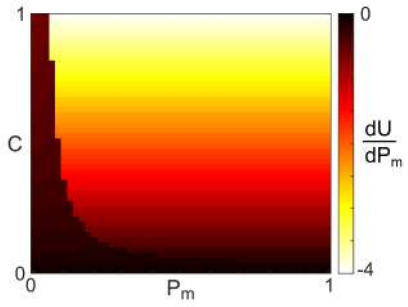

Figure S4: **Effect of increasing cooperation on stability in exploitative communities.** The derivative of stability with respect to the level of cooperation, P_m, across C/P_m parameter space reveals how increasing cooperation always destabilizes exploitative communities, regardless of the connectivity of the network that is, $\frac{dU}{dP_m} < 0$ for all values of connectivity, C, and cooperation, P_m. Here we illustrate this in a community with species number $S = 100$, and self-regulation, $-s = -1$, however, the same behavior holds true for equivalent communities with different levels of self-regulation, and higher species numbers. The two visually distinct regions of the heatmap indicate the regions where the ellipse determines stability (left) and where the dot does (right), illustrating how the dot decreases stability at a linear rate, whilst this rate is much slower in regions where community behavior is driven by the ellipse. The magnitude of $\frac{dU}{dP_m}$ is larger for higher C, indicating how increasing cooperation is more destabilizing in communities with higher connectivity.

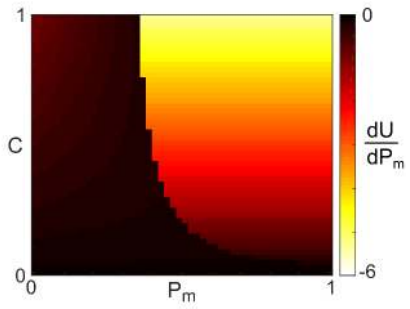

Figure S5: **Effect of increasing cooperation on stability in random communities.** The derivative of stability with respect to the level of cooperation, P_m, across C/P_m parameter space reveals how increasing cooperation always destabilizes random communities, regardless of the connectivity of the network that is, $\frac{dU}{dP_m} < 0$ for all values of connectivity, C, and cooperation, P_m. Here we illustrate this in a community with species number $S = 100$, and self-regulation, $-s = -1$, however, the same behavior holds true for equivalent communities with different levels of self-regulation, and higher species numbers. The two visually distinct regions of the heatmap indicate the regions where the ellipse determines stability (left) and where the dot does (right), illustrating how the dot decreases stability at a linear rate, whilst this rate is much slower in regions where community behavior is driven by the ellipse. The magnitude of $\frac{dU}{dP_m}$ is larger for higher C, indicating how increasing cooperation is more destabilizing in communities with higher connectivity.

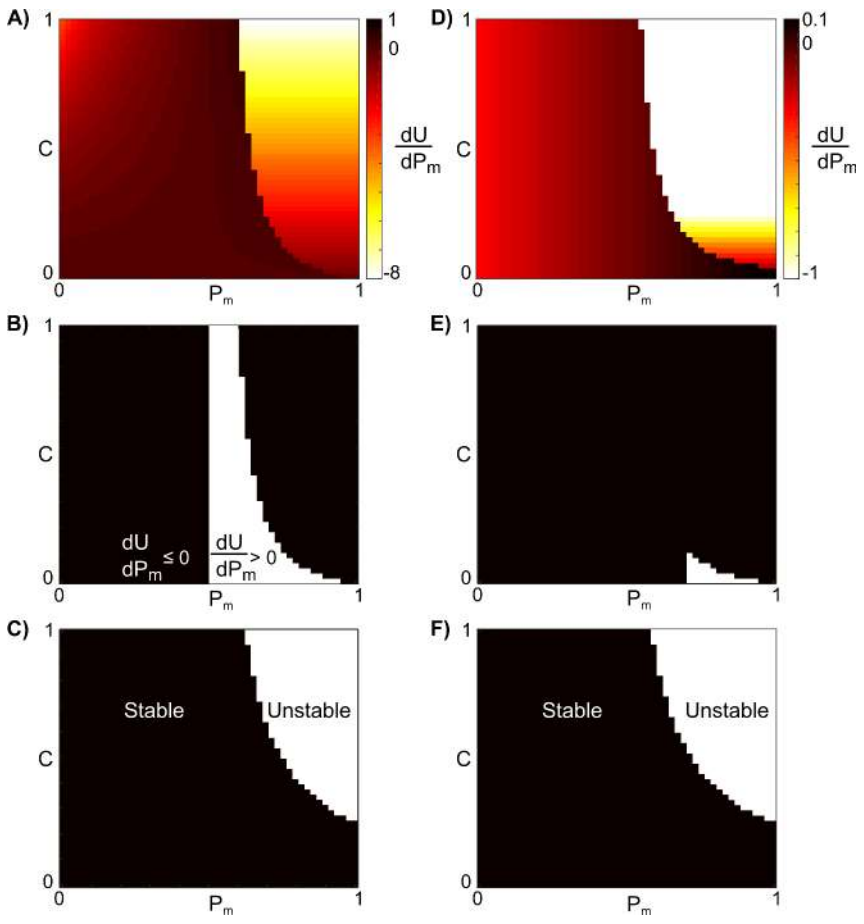

Figure S6: **Effect of cooperation on stability in competitive communities.** A) The derivative of stability with respect to the level of cooperation, P_m, across C/P_m parameter space reveals how the effect of cooperation upon stability in competitive communities changes across C/P_m parameter space. When $\frac{dU}{dP_m} < 0$ cooperation is destabilizing, whilst when $\frac{dU}{dP_m} > 0$ it is stabilizing. Note that the magnitude of the rate of stabilization is far smaller than the average rate of destabilization. B) Black regions highlight parameter space where increasing cooperation is destabilizing, whilst white regions mark where it is stabilizing. The size of the region where increasing cooperation is stabilizing decreases as connectivity, C, or species number, S, increase (here $S = 100$). C) The stabilizing influence of cooperation increase does not typically affect the transition from stable to unstable communities. This is illustrated by plots of ecological stability for a community with $S = 100, \sigma = 0.05$. D, E) In realistic communities that also contain exploitative interactions (here at 20%), the range of parameter space where increasing cooperation can be stabilizing is further reduced. F) Plot of ecological stability for communities that also contain exploitative interactions; again the stabilizing effect of increasing cooperation does not affect the stability threshold.

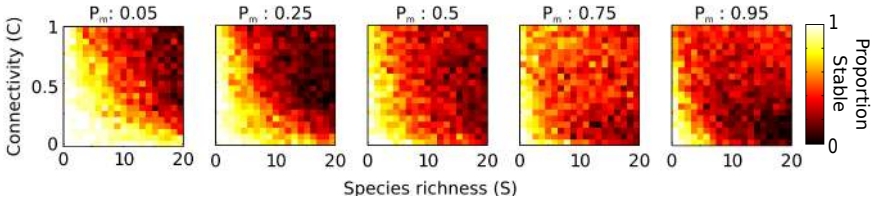

Figure S7: **Numerical confirmation that intermediate levels of cooperation (mutualism) can promote stability in a model of a macroscopic community.** We reproduce the numerical model of (*32*) in an unstructured network, and demonstrate how certain interaction dependencies can lead to increased stability for intermediate levels of cooperative interactions. Specifically, here different interaction types (cooperative versus exploitative) are weighted independently in a frequency dependent manner – such that a given species always dedicates a constant level of effort towards cooperative interactions, and a separate constant level towards exploitative interactions. As in (*32*) we numerically simulate such communities for varying values of species number, S, and connectivity, C, and plot the proportion of communities that are stable for each parameter combination in 25 independent repeats.

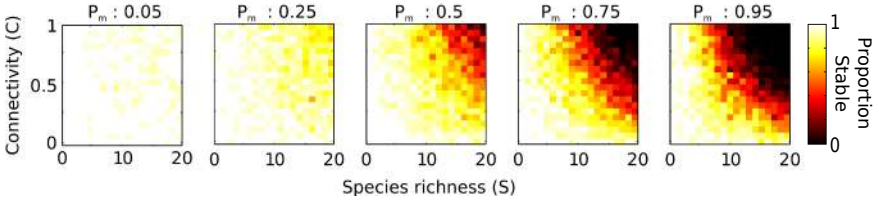

Figure S8: **Numerical confirmation that increased stability at intermediate levels of cooperation (mutualism) is not observed when each interaction type is not weighted individually.** We numerically simulate communities in S, C parameter space for varying levels of cooperative interactions (mutualism) without the frequency dependent weighting of interaction types. We simulate 25 independent communities for each parameter combination, with interaction strengths drawn from a Uniform $U([0, 0.1])$ distribution so as to, on average, be of a similar magnitude to those in Figure S7, and plot the proportion of communities that are stable.

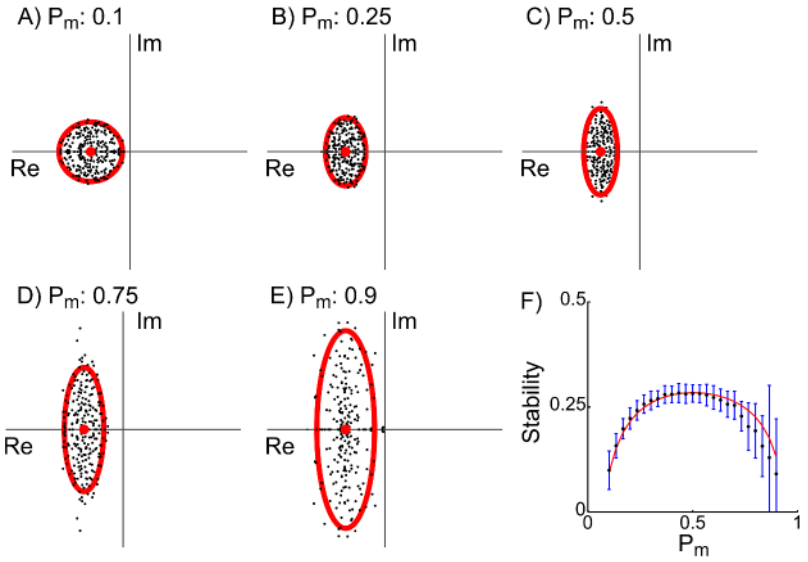

Figure S9: **Our analytical model captures the stability behavior seen numerically in (*32*).** Ecological stability is dependent upon the localization of the community's underlying eigenvalues in the complex plane. Here we demonstrate that our analytic approach can predict the change in eigenvalue localization for communities in which interactions between species are weighted in a frequency dependent manner, as in (*32*). A-E) Eigenvalues (black dots) of 4 simulated communities ($S = 100, C = 0.7$) with the frequency dependent weighting on interaction types as implemented in Figure S7 and (*32*), alongside our analytical prediction of the eigenvalue distribution (red line and dot). Some eigenvalues lie outside the ellipse because we sample interaction strengths from a random distribution, but this does not affect our ability to capture the general behavior. Panel F compares our analytical prediction of stability (red line) against the average observed stability for 100 representative networks (black dots), with blue lines representing the standard deviation. This demonstrates how our analysis can capture the behavior seen in (*32*), and our numerical simulations, when each interactions type is weighted individually.

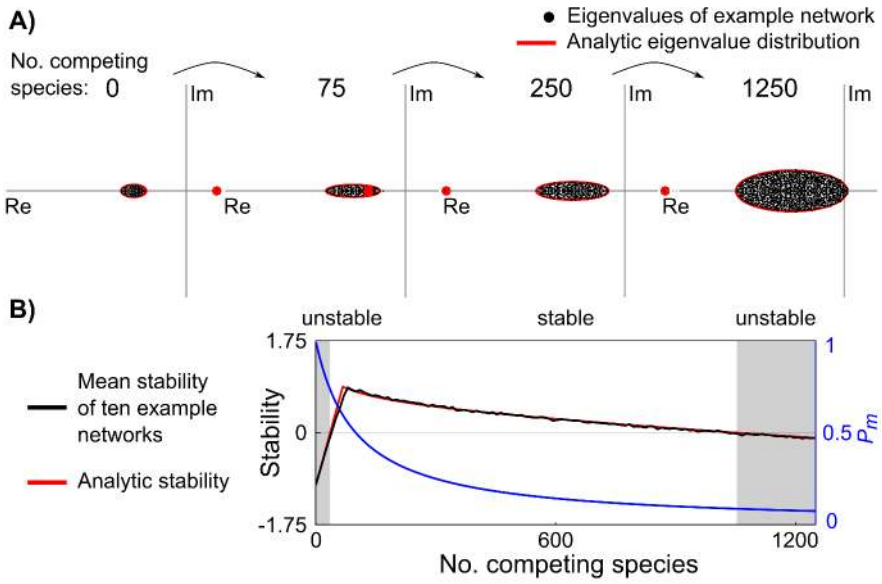

Figure S10: **Numerical confirmation of the analytical model for introducing competitive species to a network of cooperators** The stability of a community is dependent upon the localization of its eigenvalues within the complex plane, which we can predict using our analytic measure. A) We confirm the accuracy of our analytical results by numerically simulating communities in which competitive species are added to an initially purely cooperative community of 100 species ($C = 0.7, -s = -1.75, \sigma = 0.05$). We plot the eigenvalues of these simulated communities (black dots) and show how their localization is accurately predicted by our analytic bound (red line) B) We then simulate independent sample communities with different numbers of competing species, calculate their average stability (10 each, black line), and compare this with our analytical results (red line). The addition of competitors changes the proportion of cooperative links (P_m, blue line) which has a stabilizing effect that initially is stronger than the destabilizing effect of larger species numbers.

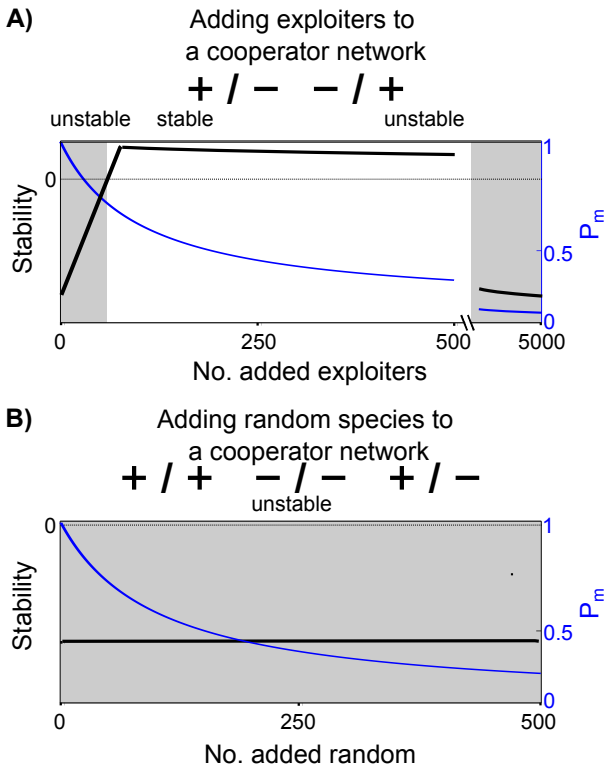

Figure S11: **Introducing exploitative species to a network of cooperators is also stabilizing, but adding random species is not**. We consider an unstable cooperative network in which all interactions are concentrated between a small number of species ($S_{\text{init}} = 100, C = 0.7, -s = -1, \sigma = 0.05$), then gradually add new species such that the original cooperative interactions are now distributed between a larger number of species. The new species interact with community members in a manner that is either exploitative (A) or "random" (B). We plot our analytic measure of stability as a function of the number of new species added (black line), and (A) demonstrate how adding exploitative species can initially stabilize the focal community, although, at high numbers of additional species, the destabilizing effect of high species numbers (Figure S1) will dominate, and the community will again destabilize. To capture this we break the plot into two sections (note the x-axis break) as the destabilizing behavior occurs at a much lower rate than the initial stabilization that occurs at low species numbers. (B) Adding species that interact in a random manner (25 % cooperatively, 25 % competitively, and 50 % exploitatively) does not have a stabilizing effect, as it does not sufficiently decrease the overall proportion of destabilizing cooperative interactions (blue line).

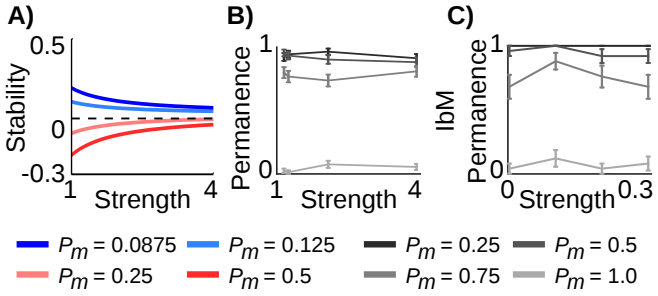

Figure S12: **Non-targeted feeding does not make communities stable.** Host-supplied nutrients that weaken all interaction types equally do not increase community stability in linear stability analysis (A), permanence analysis (B), or an individual-based model (C). In order to capture any effects of host manipulation, we study parameters for which some communities are stable and some are unstable. For linear stability analysis: $S = 300$, $C = 0.7$, $-s = -1$, $\sigma = 0.05$. For permanence analysis and IbM: $S = 10$, $-s = -0.2$, errorbars: SEM). We use different parameters for the second two methods because they are computationally expensive and can only be applied to smaller communities.

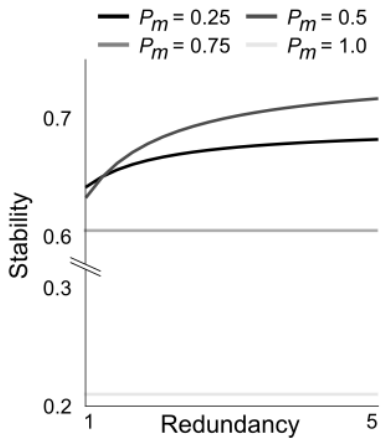

Figure S13: **Redundancy in cooperation can increase ecological stability.** We use linear stability analysis to examine the effect of replacing strong cooperative links with multiple weaker cooperative interactions. For example, one interaction of strength 1 may be replaced with three interactions, each of strength $1/3$. Whilst this manipulation does not affect highly unstable, highly cooperative communities, it can increase the stability of communities with lower levels of cooperation. The cross in the two curves for $P_m = 0.25$ and $P_m = 0.5$ occurs because the former has fewer cooperative links to make redundant and so the effects making cooperative links highly redundancy is overall weaker. We examine a network with a low initial level of connectivity, $C = 0.2$, to allow a wide range of redundancy to be examined (here: $S = 100$, $-s = -1$, $\sigma = 0.05$).

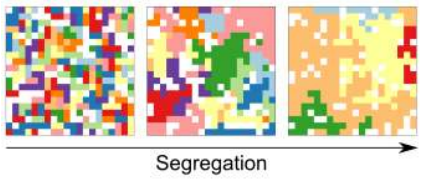

Figure S14: **Implementation of increasing spatial structure in the individual-based model.** To increase structure, we decrease the number of randomly arranged cells that start communities, which leads to the emergence of larger clonal patches. In these models, we also assume that each cell can only interact with those cells within a certain local neighborhood.

References and Notes

1. C. Lozupone, K. Faust, J. Raes, J. J. Faith, D. N. Frank, J. Zaneveld, J. I. Gordon, R. Knight, Identifying genomic and metabolic features that can underlie early successional and opportunistic lifestyles of human gut symbionts. *Genome Res.* **22**, 1974–1984 (2012). Medline doi:10.1101/gr.138198.112

2. S. R. Gill, M. Pop, R. T. Deboy, P. B. Eckburg, P. J. Turnbaugh, B. S. Samuel, J. I. Gordon, D. A. Relman, C. M. Fraser-Liggett, K. E. Nelson, Metagenomic analysis of the human distal gut microbiome. *Science* **312**, 1355–1359 (2006). Medline doi:10.1126/science.1124234

3. F. Bäckhed, R. E. Ley, J. L. Sonnenburg, D. A. Peterson, J. I. Gordon, Host-bacterial mutualism in the human intestine. *Science* **307**, 1915–1920 (2005). Medline doi:10.1126/science.1104816

4. S. K. Mazmanian, J. L. Round, D. L. Kasper, A microbial symbiosis factor prevents intestinal inflammatory disease. *Nature* **453**, 620–625 (2008). Medline doi:10.1038/nature07008

5. Y. K. Lee, S. K. Mazmanian, Has the microbiota played a critical role in the evolution of the adaptive immune system? *Science* **330**, 1768–1773 (2010). Medline doi:10.1126/science.1195568

6. L. Dethlefsen, D. A. Relman, Incomplete recovery and individualized responses of the human distal gut microbiota to repeated antibiotic perturbation. *Proc. Natl. Acad. Sci. U.S.A.* **108** (suppl. 1), 4554–4561 (2011). Medline doi:10.1073/pnas.1000087107

7. T. Vanhoutte, G. Huys, E. Brandt, J. Swings, Temporal stability analysis of the microbiota in human feces by denaturing gradient gel electrophoresis using universal and group-specific 16S rRNA gene primers. *FEMS Microbiol. Ecol.* **48**, 437–446 (2004). Medline doi:10.1016/j.femsec.2004.03.001

8. J. J. Faith, J. L. Guruge, M. Charbonneau, S. Subramanian, H. Seedorf, A. L. Goodman, J. C. Clemente, R. Knight, A. C. Heath, R. L. Leibel, M. Rosenbaum, J. I. Gordon, The long-term stability of the human gut microbiota. *Science* **341**, 1237439 (2013). Medline doi:10.1126/science.1237439

9. D. A. Relman, The human microbiome: Ecosystem resilience and health. *Nutr. Rev.* **70** (suppl. 1), S2–S9 (2012). Medline doi:10.1111/j.1753-4887.2012.00489.x

10. A. Giongo, K. A. Gano, D. B. Crabb, N. Mukherjee, L. L. Novelo, G. Casella, J. C. Drew, J. Ilonen, M. Knip, H. Hyöty, R. Veijola, T. Simell, O. Simell, J. Neu, C. H. Wasserfall, D. Schatz, M. A. Atkinson, E. W. Triplett, Toward defining the autoimmune microbiome for type 1 diabetes. *ISME J.* **5**, 82–91 (2011). Medline

11. C. A. Lozupone, J. I. Stombaugh, J. I. Gordon, J. K. Jansson, R. Knight, Diversity, stability and resilience of the human gut microbiota. *Nature* **489**, 220–230 (2012). Medline doi:10.1038/nature11550

12. P. De Cruz, L. Prideaux, J. Wagner, S. C. Ng, C. McSweeney, C. Kirkwood, M. Morrison, M. A. Kamm, Characterization of the gastrointestinal microbiota in health and inflammatory bowel disease. *Inflamm. Bowel Dis.* **18**, 372–390 (2012). Medline doi:10.1002/ibd.21751

13. E. Y. Hsiao, S. W. McBride, S. Hsien, G. Sharon, E. R. Hyde, T. McCue, J. A. Codelli, J. Chow, S. E. Reisman, J. F. Petrosino, P. H. Patterson, S. K. Mazmanian, Microbiota modulate behavioral and physiological abnormalities associated with neurodevelopmental disorders. *Cell* **155**, 1451–1463 (2013). Medline doi:10.1016/j.cell.2013.11.024

14. J. Schluter, K. R. Foster, The evolution of mutualism in gut microbiota via host epithelial selection. *PLOS Biol.* **10**, e1001424 (2012). Medline doi:10.1371/journal.pbio.1001424

15. V. Bucci, S. Bradde, G. Biroli, J. B. Xavier, Social interaction, noise and antibiotic-mediated switches in the intestinal microbiota. *PLOS Comput. Biol.* **8**, e1002497 (2012). Medline doi:10.1371/journal.pcbi.1002497

16. R. R. Stein, V. Bucci, N. C. Toussaint, C. G. Buffie, G. Rätsch, E. G. Pamer, C. Sander, J. B. Xavier, Ecological modeling from time-series inference: Insight into dynamics and stability of intestinal microbiota. *PLOS Comput. Biol.* **9**, e1003388 (2013). Medline doi:10.1371/journal.pcbi.1003388

17. R. M. May, Will a large complex system be stable? *Nature* **238**, 413–414 (1972). Medline doi:10.1038/238413a0

18. S. Allesina, S. Tang, Stability criteria for complex ecosystems. *Nature* **483**, 205–208 (2012). Medline doi:10.1038/nature10832

19. K. S. McCann, The diversity-stability debate. *Nature* **405**, 228–233 (2000). Medline doi:10.1038/35012234

20. K. R. Foster, T. Bell, Competition, not cooperation, dominates interactions among culturable microbial species. *Curr. Biol.* **22**, 1845–1850 (2012). Medline doi:10.1016/j.cub.2012.08.005

21. G. Eberl, A new vision of immunity: Homeostasis of the superorganism. *Mucosal Immunol.* **3**, 450–460 (2010). Medline doi:10.1038/mi.2010.20

22. R. D. Sleator, The human superorganism - of microbes and men. *Med. Hypotheses* **74**, 214–215 (2010). Medline doi:10.1016/j.mehy.2009.08.047

23. P. Van den Abbeele, T. Van de Wiele, W. Verstraete, S. Possemiers, The host selects mucosal and luminal associations of coevolved gut microorganisms: A novel concept. *FEMS Microbiol. Rev.* **35**, 681–704 (2011). Medline doi:10.1111/j.1574-6976.2011.00270.x

24. R. Di Cagno, M. De Angelis, I. De Pasquale, M. Ndagijimana, P. Vernocchi, P. Ricciuti, F. Gagliardi, L. Laghi, C. Crecchio, M. E. Guerzoni, M. Gobbetti, R. Francavilla, Duodenal and faecal microbiota of celiac children: Molecular, phenotype and metabolome characterization. *BMC Microbiol.* **11**, 219 (2011). Medline doi:10.1186/1471-2180-11-219

25. F. Fiegna, G. J. Velicer, Exploitative and hierarchical antagonism in a cooperative bacterium. *PLOS Biol.* **3**, e370 (2005). Medline doi:10.1371/journal.pbio.0030370

26. J. C. Clemente, E. C. Pehrsson, M. J. Blaser, K. Sandhu, Z. Gao, B. Wang, M. Magris, G. Hidalgo, M. Contreras, Ó. Noya-Alarcón, O. Lander, J. McDonald, M. Cox, J. Walter, P. L. Oh, J. F. Ruiz, S. Rodriguez, N. Shen, S. J. Song, J. Metcalf, R. Knight, G. Dantas, M.

G. Dominguez-Bello, The microbiome of uncontacted Amerindians. *Sci. Adv.* **1**, e1500183 (2015). Medline doi:10.1126/sciadv.1500183

27. N. M. Oliveira, R. Niehus, K. R. Foster, Evolutionary limits to cooperation in microbial communities. *Proc. Natl. Acad. Sci. U.S.A.* **111**, 17941–17946 (2014). doi:10.1073/pnas.1412673111

28. B. S. Samuel, J. I. Gordon, A humanized gnotobiotic mouse model of host-archaeal-bacterial mutualism. *Proc. Natl. Acad. Sci. U.S.A.* **103**, 10011–10016 (2006). Medline doi:10.1073/pnas.0602187103

29. E. P. Wigner, On the distribution of the roots of certain symmetric matrices. *Ann. Math.* **67**, 325–327 (1958). doi:10.2307/1970008

30. H. J. Sommers, A. Crisanti, H. Sompolinsky, Y. Stein, Spectrum of large random asymmetric matrices. *Phys. Rev. Lett.* **60**, 1895–1898 (1988). Medline doi:10.1103/PhysRevLett.60.1895

31. See the supplementary materials on *Science* Online.

32. A. Mougi, M. Kondoh, Diversity of interaction types and ecological community stability. *Science* **337**, 349–351 (2012). Medline doi:10.1126/science.1220529

33. R. P. Rohr, S. Saavedra, J. Bascompte, On the structural stability of mutualistic systems. *Science* **345**, 1253497 (2014). Medline doi:10.1126/science.1253497

34. P. Louis, G. L. Hold, H. J. Flint, The gut microbiota, bacterial metabolites and colorectal cancer. *Nat. Rev. Microbiol.* **12**, 661–672 (2014). Medline doi:10.1038/nrmicro3344

35. C. S. Holling, Resilience and stability of ecological systems. *Annu. Rev. Ecol. Syst.* **4**, 1–23 (1973). doi:10.1146/annurev.es.04.110173.000245

36. M. Kondoh, A. Mougi, Interaction-type diversity hypothesis and interaction strength: The condition for the positive complexity-stability effect to arise. *Popul. Ecol.* **57**, 21–27 (2015). doi:10.1007/s10144-014-0475-9

37. X. Chen, J. E. Cohen, Global stability, local stability and permanence in model food webs. *J. Theor. Biol.* **212**, 223–235 (2001). Medline doi:10.1006/jtbi.2001.2370

38. W. Jansen, A permanence theorem for replicator and Lotka-Volterra systems. *J. Math. Biol.* **25**, 411–422 (1987). doi:10.1007/BF00277165

39. A. S. Waller, T. Yamada, D. M. Kristensen, J. R. Kultima, S. Sunagawa, E. V. Koonin, P. Bork, Classification and quantification of bacteriophage taxa in human gut metagenomes. *ISME J.* **8**, 1391–1402 (2014). Medline doi:10.1038/ismej.2014.30

40. J. Hofbauer, K. Sigmund, On the stabilizing effect of predators and competitors on ecological communities. *J. Math. Biol.* **27**, 537–548 (1989). Medline doi:10.1007/BF00288433

41. J. K. Fredrickson, Ecological communities by design. *Science* **348**, 1425–1427 (2015). Medline doi:10.1126/science.aab0946

42. H. J. Kim, J. Q. Boedicker, J. W. Choi, R. F. Ismagilov, Defined spatial structure stabilizes a synthetic multispecies bacterial community. *Proc. Natl. Acad. Sci. U.S.A.* **105**, 18188–18193 (2008). Medline doi:10.1073/pnas.0807935105

43. L. V. Hooper, J. Xu, P. G. Falk, T. Midtvedt, J. I. Gordon, A molecular sensor that allows a gut commensal to control its nutrient foundation in a competitive ecosystem. *Proc. Natl. Acad. Sci. U.S.A.* **96**, 9833–9838 (1999). Medline doi:10.1073/pnas.96.17.9833

44. P. C. Kashyap, A. Marcobal, L. K. Ursell, S. A. Smits, E. D. Sonnenburg, E. K. Costello, S. K. Higginbottom, S. E. Domino, S. P. Holmes, D. A. Relman, R. Knight, J. I. Gordon, J. L. Sonnenburg, Genetically dictated change in host mucus carbohydrate landscape exerts a diet-dependent effect on the gut microbiota. *Proc. Natl. Acad. Sci. U.S.A.* **110**, 17059–17064 (2013). Medline

45. J. L. Sonnenburg, J. Xu, D. D. Leip, C. H. Chen, B. P. Westover, J. Weatherford, J. D. Buhler, J. I. Gordon, Glycan foraging in vivo by an intestine-adapted bacterial symbiont. *Science* **307**, 1955–1959 (2005). Medline doi:10.1126/science.1109051

46. V. Tremaroli, F. Bäckhed, Functional interactions between the gut microbiota and host metabolism. *Nature* **489**, 242–249 (2012). Medline doi:10.1038/nature11552

47. F. H. Login, S. Balmand, A. Vallier, C. Vincent-Monégat, A. Vigneron, M. Weiss-Gayet, D. Rochat, A. Heddi, Antimicrobial peptides keep insect endosymbionts under control. *Science* **334**, 362–365 (2011). Medline doi:10.1126/science.1209728

48. D. Haydon, Pivotal assumptions determining the relationship between stability and complexity: An analytical synthesis of the stability-complexity debate. *Am. Nat.* **144**, 14–29 (1994). doi:10.1086/285658

49. D. R. Nemergut, S. K. Schmidt, T. Fukami, S. P. O'Neill, T. M. Bilinski, L. F. Stanish, J. E. Knelman, J. L. Darcy, R. C. Lynch, P. Wickey, S. Ferrenberg, Patterns and processes of microbial community assembly. *Microbiol. Mol. Biol. Rev.* **77**, 342–356 (2013). Medline doi:10.1128/MMBR.00051-12

50. S. Mitri, K. R. Foster, The genotypic view of social interactions in microbial communities. *Annu. Rev. Genet.* **47**, 247–273 (2013). Medline doi:10.1146/annurev-genet-111212-133307

51. S. Gerschgorin, Über die Abgrenzung der Eigenwerte einer Matrix. *B. Acad. Sci. USSR* **25**, 750–754 (1931).

52. T. Tao, V. Vu, M. Krishnapur, Random matrices: Universality of ESDs and the circular law. *Ann. Probab.* **38**, 2023–2065 (2010). doi:10.1214/10-AOP534

53. U. G. Rothblum, C. P. Tan, Upper bounds on the maximum modulus of subdominant eigenvalues of nonnegative matrices. *Linear Algebra Appl.* **66**, 45–86 (1985). doi:10.1016/0024-3795(85)90125-9

54. B. S. Goh, Stability in models of mutualism. *Am. Nat.* **113**, 261–275 (1979). doi:10.1086/283384